Determining Water Storage Depletion within Iran by Assimilating GRACE data into the W3RA Hydrological Model

M. Khaki[a,1], E. Forootan[b], M. Kuhn[a], J. Awange[a], A. I. J. M. van Dijk[c], M. Schumacher[d], M. A. Sharifi[e,f]

[a]*School of Earth and Planetary Sciences, Discipline of Spatial Sciences, Curtin University, Perth, Australia.*
[b]*School of Earth and Ocean Sciences, Cardiff University, Cardiff, UK.*
[c]*Fenner School of Environment and Society, the Australian National University, Canberra, Australia.*
[d]*School of Geographical Sciences, University of Bristol, Bristol, UK.*
[e]*Faculty of Surveying and Geospatial Engineering, College of Engineering, University of Tehran, Iran.*
[f]*Research Institute of Geoinformation Technology (RIGT), College of Engineering, University of Tehran, Iran.*

Abstract

Groundwater depletion, due to both unsustainable water use and a decrease in precipitation, has been reported in many parts of Iran. In order to analyze these changes during the recent decade, in this study, we assimilate Terrestrial Water Storage (TWS) data from the Gravity Recovery And Climate Experiment (GRACE) into the World-Wide Water Resources Assessment (W3RA) model. This assimilation improves model derived water storage simulations by introducing missing trends and correcting the amplitude and phase of seasonal water storage variations. The Ensemble Square-Root Filter (EnSRF) technique is applied, which showed stable performance in propagating errors during the assimilation period (2002-2012). Our focus is on sub-surface water storage changes including groundwater and soil moisture variations within six major drainage divisions covering the whole Iran including its eastern part (East), Caspian Sea, Centre, Sarakhs, Persian Gulf and Oman Sea, and Lake Urmia. Results indicate an average of -8.9 mm/year groundwater reduction within Iran during the period 2002 to 2012. A similar decrease is also observed in soil moisture storage especially after 2005. We further apply the canonical correlation analysis (CCA) technique to relate sub-surface water storage changes to climate (e.g., precipitation) and anthropogenic (e.g., farming) impacts. Results indicate an average correlation of 0.81 between rainfall and groundwater variations and also a large impact of anthropogenic activities (mainly for irrigations) on Iran's water storage depletions.

Keywords: Iran, Groundwater Storage, Data Assimilation, Canonical Correlation Analysis, GRACE, W3RA Hydrological Model, Water Storage Depletion

Email address: Mehdi.Khaki@postgrad.curtin.edu.au (M. Khaki)
[1]Contact details: Department of Spatial Sciences, Curtin University, Perth, Australia, Email: Mehdi.Khaki@postgrad.curtin.edu.au, Tel: 0061410620379

1. Introduction

Water scarcity has become a serious issue in the Islamic Republic of Iran (abbreviated here as Iran) in recent years (e.g., Amery and Wolf, 2000; Wolf and Newton, 2007; Trigo et al., 2010; Madani, 2014; Michel, 2017). With the increased extraction of groundwater, its level has been reported to fall significantly (see, e.g., Sarraf et al., 2005; Motagh et al., 2008; Mohammadi-Ghaleni and Ebrahimi, 2011; Van Camp et al., 2012; Afshar et al., 2016). There have been studies that investigate surface and groundwater changes in Iran during the last decade (2003 onward) mainly using Terrestrial Water Storage (TWS) data from the Gravity Recovery And Climate Experiment (GRACE, Tapley et al., 2004). For example, Voss et al. (2013) reported $\sim$143.6 km^3 reduction of freshwater from 2003 to 2009 over the north-central area of the Middle East, which largely covers the Tigris-Euphrates Basin. Forootan et al. (2014a) applied a statistical inversion to separate GRACE TWS using hydrological model outputs and altimetry data as a priori information, and found a decrease in water storage with an average linear rate of $\sim$-15 mm/year between 2002 and 2011. A large negative trend (2003-2012) in TWS was observed by Joodaki et al. (2014) using GRACE TWS data over the western Iran and eastern Iraq.

Estimating sub-surface water storages is very important since they support the life in semi-arid areas like Iran. Fatolazadeh et al. (2016) used the wavelet approach to improve estimates of groundwater storage variations from GRACE and found a remarkable decrease in groundwater in 2008, 2010 and particularly in 2011. Forootan et al. (2017) compared changes in water storage and hydrological water fluxes in Iran using GRACE and climate reanalysis data. Their results indicated that the decline of TWS in the Urmia and Tigris-Euphrates basins are greater than the decrease in the monthly accumulated total water fluxes. Therefore, it was concluded that the anthropogenic contribution on surface and groundwater flow is significant, and results in the storage decline within Iran.

These studies have proved the effectiveness of GRACE to enhance the understanding of water storage changes within the country. However, they do not provide a full understanding of spatially distributed water resources changes in different water compartments in Iran. GRACE TWS measures the summation of all water masses in the surface and sub-surface compartment of the terrestrial water storage (vegetation, snow, surface waters, soil, groundwater, etc.). Therefore, GRACE TWS must be separated into different storage compartments, which has been achieved to date through a forward modeling or an inversion framework as is described in

Forootan et al. (2014a) and the literature mentioned before.

To complement previous attempts, the aims of this study are to (i) update hydrological model simulations of sub-surface water storage changes (including water stored in the soil and groundwater storage) within Iran using GRACE data assimilation, and (ii) investigate climate and anthropogenic impacts on the estimated sub-surface water storages in (i). This study is the first data assimilation attempt to integrate GRACE TWS into the World-Wide Water Resources Assessment (W3RA; van Dijk, 2010) hydrological model over Iran. This methodology has been implemented in studies to constrain the mass balance of hydrological models over different river basins (e.g., Zaitchik et al., 2008; van Dijk et al., 2014; Eicker et al., 2014; Reager et al., 2015; Girotto et al., 2016; Schumacher et al., 2016). The main rationale in following this approach is that one relies on the physical processes, implemented in the model equations, to separate GRACE TWS into water compartments (see similar arguments, e.g., in Bertino et al., 2003). Thus, by generating ensemble members for a model derived water storage simulation, we will compute a priori estimates of mass redistribution in the country. Then, by assimilating GRACE data, while considering their uncertainty, we update (correct) these model estimations. A similar concept has also been followed in studies in hydrology, climate, and oceanography (see, e.g., Garner et al., 1999; Bennett, 2002; Kalnay, 2003; Schunk et al., 2004; Lahoz et al., 2007; Khaki et al., 2017a,b). In addition, by applying data assimilation, we will likely be able to reliably separate GRACE TWS data into different water compartments since both model and observation errors are considered. Considering that the spatial resolution of models is usually better than GRACE data, through the assimilation procedure, GRACE observations are downscaled, and therefore, higher resolution estimations of water storages will be available within the country (see also Schumacher et al., 2016; Khaki et al., 2018a).

Once improved model simulations are obtained, by assimilating GRACE TWS, relationships between the model-derived groundwater and soil moisture storages and climatic variables within Iran are investigated. To investigate the impacts of climate on the regional water storage estimates, precipitation from satellite remote sensing, temperature, and vegetation changes through the Normalized Difference Vegetation Index (NDVI) are used. Furthermore, anthropogenic effects are explored using the changes in water use for farming, industry, and human consumption. To this end, Canonical Correlation Analysis (CCA) is applied to provide an insight into the relations between model-derived water storages and both climatic and anthropogenic impacts by extracting spatio-temporal correlations between these inter-related data

sets. For a better spatial analysis of water storage and to reduce the uncertainty of estimations, the study area is divided into six major areas: the eastern part of Iran (indicated by East), Caspian Sea, Centre, Sarakhs, Persian Gulf and Oman Sea, and Lake Urmia (Figure 1).

The remainder of this study is structured as follows: Section 2 provides details on W3RA model, remotely sensed datasets, and in-situ measurements used. In Section 3, data assimilation filtering techniques, CCA algorithm, and the outline of our experimental setup are described. Results are presented and discussed in Section 4 including the data assimilation performance and analyzing the relationship between the model estimations, rainfall and NDVI through CCA. Finally, the study is concluded in Section 5.

FIGURE 1

2. Study area and data

2.1. Iran

Located in an arid and semi-arid region, Iran experiences strong regional differences in climate (Figure 1). Subtropical conditions are dominant over the northern part, but 90% of the country has limited rainfall with extremely hot summers in the central and southern coastal regions (Golian et al., 2015). Much of the west to northwest of Iran is located in high plateaus and mountain ranges associated with strong temperature differences between winter and summer. By contrast, the centre to southern parts are warm (cf. Figure 1) for most of the year with mild winters and hot summers. Annual rainfall, the main source of freshwater in Iran, varies from 50 mm in the deserts to 2275 mm in the northern part of the country (FAO, 2009). Only a fraction of the country receives enough rainfall for agriculture. A growing use of irrigation for agricultural productions (Ardakani, 2009) and the increasing population (from ∼55 million in 1990 to ∼80 million in 2015 Karamouzian and Haghdoost, 2015), make water availability an important issue across the country (Michel, 2017).

2.2. W3RA hydrological model

The present study uses the globally distributed World-Wide Water Resources Assessment system (W3RA) model, run at $1^\circ \times 1^\circ$. W3RA, based on the Australian Water Resources Assessment system (AWRA) model (version 0.5) developed in 2008 by the Commonwealth Scientific and Industrial Research Organization (CSIRO) is a daily grid-distributed biophysical

model that simulates landscape water stored in the vegetation and soil systems (see details in van Dijk, 2010). The model represent and forecast terrestrial water cycles (van Dijk, 2010; Renzullo et al., 2014). W3RA does not consider anthropogenic effects (e.g., irrigation). Therefore, by assimilating GRACE TWS, which integrates both natural and anthropogenic signals (e.g., Schumacher et al., 2018), we hope to constrain the model's water storage simulations and introduce the missing variations. Meteorological forcing data that is used here are minimum and maximum temperature, down-welling short-wave radiation, and precipitation from the Princeton University (Sheffield et al., 2006). The model contains effective soil parameters, water holding capacity and soil evaporation, relating greenness and groundwater recession, and saturated area to catchment characteristics parameters (van Dijk et al., 2013). This one-dimensional grid-based water balance model represents the water balance of the soil, groundwater and surface water stores in which each cell is modeled independently of its neighbors (van Dijk, 2010; Renzullo et al., 2014). The model state, which is used for data assimilation (2002-2012), is composed of W3RA storages of the top, shallow root and deep root soil layers, and groundwater storage in an one-dimensional system (vertical variability).

2.2.1. Satellite-derived observations

We use monthly GRACE level 2 (L2) gravitational Stokes' coefficients truncated up to spherical harmonic degree and order 90 along with their full error information from 2002 to 2012 provided by the ITSG-Grace2016 gravity field model (Mayer-Gürr et al., 2014). The monthly full error information of the Stokes' coefficients is used to construct an observation error covariance matrix for the GRACE TWS fields to be used for data assimilation (Schumacher et al., 2016). Degree 1 of Stokes' coefficients are replaced with those estimated by Swenson et al. (2008) to account for the movement of the Earth's center of mass. Degree 2 and order 0 (C20) coefficients are replaced by those from Satellite Laser Ranging solutions due to unquantified large uncertainties in this term (e.g., Cheng and Tapley, 2004; Chen et al., 2007). Afterward, following Wahr et al. (1998), the L2 gravity fields is converted to gridded TWS fields with a $1^\circ \times 1^\circ$ spatial resolution.

Correlated noise in data due to anisotropic spatial sampling, instrumental noise (K-band ranging system and GPS), and temporal aliasing caused by the incomplete reduction of short-term mass variations (Forootan et al., 2014b) can be reduced by smoothing filters (e.g., Kusche et al., 2009). The application of smoothing, however, causes a spatial leakage problem that can

be problematic given that strong water resources of Tigris River and the Persian Gulf Basin can affect GRACE signals, as leakage-in errors, over the northwest and south of Iran, respectively. To tackle these errors, we use a Kernel Fourier Integration (KeFIn) filter, proposed by Khaki et al. (2018b), which defines an efficient averaging kernel to improve GRACE TWS within Iran. The KeFIn filtering method accounts for signal attenuations and leakage effects caused by smoothing in a two step filtering scheme (see more details in Khaki et al., 2018b). Lastly, in order to reach absolute TWS estimates (similar to W3RA), the mean TWS for the study period is taken from W3RA and added to the GRACE TWS anomalies time series.

Furthermore, since W3RA does not simulate lake dynamics, one needs to account for the existing surface water storage over the Lake Urmia before assimilation of the GRACE TWS data. Water level height datasets from satellite radar altimetry of Jason-1 (260 cycles from 2002 to 2008) and Jason-2 (165 cycles from 2008 to 2012) are used to separate groundwater and surface water storage from GRACE TWS (more details in Section 3.1.2). We use the ExtR post-processing technique (Khaki et al., 2014, 2015) to retrack the data and improve water level measurements, which are erroneous within inland waters. Filtered surface heights are then used to create time series for virtual gauge stations over the Lake Urmia. These time series are subsequently used to remove the contribution of surface water storage changes from GRACE TWS data before implementing the proposed data assimilation (see also the procedure in Forootan et al., 2014a).

Satellite-derived precipitation data of TRMM-3B43 products (TRMM, 2011) from the Tropical Rainfall Measuring Mission Project (TRMM; version 7) is used to study rainfall variations. We convert the gridded precipitation products provided with a $0.25^\circ \times 0.25^\circ$ spatial scale to $1^\circ \times 1^\circ$ for the period between 2002 and 2012. In addition, we use Version 4 gridded daily Normalized Difference Vegetation Index (NDVI) derived from the NOAA Climate Data Record (CDR) between 2002 and 2012 to further investigate climatic impacts. This dataset is produced by the NASA Goddard Space Flight Center (GSFC) and the University of Maryland with a $0.05^\circ \times 0.05^\circ$ spatial resolution. The datasets are rescaled to a $1^\circ \times 1^\circ$ spatial resolution. A summary of the data sets and links to download the data are provided in Table 1.

2.2.2. Temperature

Monthly average temperature data for the temporal period of 2003 to 2012 is acquired from Climatic Research Unit (CRU; Harris, 2008), which is used in CCA as a climate indicator.

This data is provided using more than 4000 weather stations distributed around the world. For the sake of consistency with other data sets, the collected $0.5^\circ \times 0.5^\circ$ spatial scale data is converted to $1^\circ \times 1^\circ$.

2.3. In-situ data

We use in-situ groundwater level data collected from 562 observation wells distributed over the six drainage divisions of East, Caspian Sea, Centre, Sarakhs, Persian Gulf and Oman Sea, and Lake Urmia water (cf. Figures 1) to compare them with our results. Datasets are provided by the Iran Water Resources Management Company (IWRMC) and are categorized based on Iran's six largest provinces on a yearly temporal scale presenting groundwater storage changes for an entire aquifer (Forootan et al., 2014a). Figure 2 shows an annual increase in groundwater extraction and the number of drilled wells for the entire country derived from IWRMC data sets. The IWRMC volumetric groundwater change measurements are converted to equivalent water height using the area of each aquifer. The area-averaged time series of groundwater changes for each aquifer is then generated and used for evaluating the results. The modified in-situ groundwater time series are compared separately to the average assimilation results for the same aquifer. River water discharge, the number of bore holes, and average water use for farming, industry, and urban use provided by IWRMC are also used in the CCA process (see Section 3.2). Details of all the applied datasets, as well as the model are presented in Table 1.

FIGURE 2

TABLE 1

3. Method

3.1. Data assimilation

3.1.1. EnSRF filtering

In order to assimilate GRACE data into the W3RA model, we use the Ensemble Square-Root Filter (EnSRF) following Whitaker and Hamill (2002). EnSRF is an extended version of traditional Ensemble Kalman Filter (EnKF) that does not require the observations to be perturbed by introducing a new sampling scheme. Here, EnSRF is selected to avoid sampling

errors that can be reflected in the background covariance matrix especially in using a limited number of ensembles (Whitaker and Hamill, 2002). Khaki et al. (2017a) showed that this method is highly capable of assimilating GRACE TWS data into a hydrological model amongst the most commonly used filters. EnSRF adopts a similar analysis step to the EnKF in the sense that the analysis perturbations are computed from the forecast perturbations by updating each ensemble perturbation with a Kalman-like update step. In the present study X consists of six different water storages including top soil, shallow soil, and deep soil water, vegetation, snow, and groundwater storages. Previous studies, e.g., Forootan et al. (2014a) and Tourian et al. (2015), have investigated the surface water variations, specifically, in the Lake Urmia Basin and the Caspian Sea as the major source of surface water storage changes in Iran. Therefore, here, we only focus on the estimation of sub-surface compartments including groundwater and soil moisture. The modified GRACE TWS data (see Section 2.2.1 for details) is then used to update the above water compartments excluding surface storage.

The forecast model state, the integrated model state by a dynamical model for N times (N is the ensemble number), is represented by $X^f = [{X_1}^f \dots {X_N}^f]$, where ${X_i}^f$ $(i = 1 \dots N)$ is the ith ensemble (hereafter 'f' refers to forecast and 'a' represents analysis). The corresponding model state forecast error covariance of P^f is defined by:

$$P^f = \frac{1}{N-1} \sum_{i=1}^{N} ({X_i}^f - \bar{X}^f)({X_i}^f - \bar{X}^f)^T, \tag{1}$$

$$\bar{X}^f = \frac{1}{N} \sum_{i=1}^{N} (X_i). \tag{2}$$

The update stage in EnSRF contains two steps. First, it updates the ensemble-mean following,

$$\bar{X}^a = \bar{X}^f + K(y - H\bar{X}^f), \quad i = 1 \dots N, \tag{3}$$

$$K = P^f (H)^T (HP^f (H)^T + R)^{-1}, \tag{4}$$

where K is the Kalman gain, y is the observation vector. The transition matrix and the observation covariance matrix are indicated by H and R, respectively. Next, EnSRF updates the forecast ensemble of anomalies $A^f = [{A_1}^f \dots {A_N}^f]$ into the analysis ensemble deviation A^a. A^f as the deviation of model state ensembles from the ensemble mean is derived from,

$${A_i}^f = {X_i}^f - \bar{X}^f. \tag{5}$$

EnSRF exploits the serial formulation of the Kalman filter analysis step in which the observations are assimilated each at a time to compute the analysis perturbations that exactly match the Kalman filter covariance (Hoteit et al., 2008) using the modified gain ($\tilde{K}$) with,

$$A^a = (I - \tilde{K}H)A_i{}^f, \tag{6}$$

$$\alpha = \left(1 + \sqrt{\frac{R}{HP^fH^T + R}}\right)^{-1}, \tag{7}$$

where I is an identity matrix. More details on EnSRF can be found in Whitaker and Hamill (2002) and Tippett et al. (2003).

3.1.2. Assimilating GRACE TWS into W3RA

Monthly gridded GRACE TWS data are assimilated into W3RA to update the model states, a summation of model vertical water compartments (here soil moisture, vegetation biomass, snow, and groundwater). Note that no parameter adjustment is considered here and the observations are only used to constrain the system states. The monthly increment (i.e., the difference between the monthly averaged GRACE TWS and simulated TWS) can be added to each day of the current month, which guarantees that the update of the monthly mean is identical to the monthly mean of the daily updates. In practice, the differences between the predictions and the updated states are added as offsets to the state vectors at the last day of each month to generate the ensembles for the next month assimilation step. We use Monte Carlo sampling of multivariate normal distributions with the errors representing the standard deviations of the forcing sets (precipitation, temperature, and radiation) to generate an initial ensemble (Renzullo et al., 2014). The perturbed meteorological forcing datasets, then, are integrated forward with the model from 2000 to 2002 providing 72 sets of state vectors (as suggested by Oke et al., 2008) at the beginning of the study period.

An application of small ensemble size is problematic in ensemble data assimilation systems, as it can lead to filter divergent or inaccurate estimation (Tippett et al., 2003). Therefore, we apply ensemble inflation that uses a small coefficient factor (here 1.12; Anderson et al., 2001) to inflate prior ensemble deviation from the ensemble-mean and increases their variations (Anderson et al., 2007). Furthermore, the Local Analysis (LA) scheme (Evensen, 2003; Ott et al., 2004) is applied for localization. LA improves the assimilation procedure by restricting the

observations used for the covariance matrix computation to a spatially limited area (Khaki et al., 2017c). As a result, only those measurements located within a certain distance from a grid point have an impact on the updated states (Evensen, 2003; Ott et al., 2004). Different localization lengths are tested and their results are assessed against in-situ groundwater measurements (Section 2.3) to reach the best case scenario (i.e., 5° half-width used in this study).

As mentioned, it is necessary to remove surface water storages from GRACE TWS data over Lake Urmia before data assimilation. For this purpose, following Forootan et al. (2014a) who undertook water analysis over the same area, we use satellite altimetry time series over the lake to derive surface water storage. The Global Land Data Assimilation System (GLDAS) outputs of total column soil moisture, snow water equivalent, and vegetation biomass water storage as well as water level variations from altimetry are used to estimate temporal and spatial patterns of surface water storage using Independent Component Analysis (ICA). The extracted patterns are then adjusted to GRACE TWS products using a least squares adjustment (LSA) procedure (see details in Forootan et al., 2014a). The GRACE data after removing surface water storage is used for the data assimilation process over Lake Urmia.

3.2. Canonical Correlation Analysis (CCA)

The present study applies Canonical Correlation Analysis (CCA) to find the linear connection of two sets of multidimensional variables of predictor (x_c) and criterion (y_c) values. CCA is selected here rather than simple correlation analysis due to its ability in establishing the relationships between multiple intercorrelated variables. CCA extracts canonical coefficients that represent common processes between two or more variables (Chang et al., 2013) using an eigenvector decomposition that yields linear weights, known as canonical coefficients, which describe maximum correlations between variables (see details in Steiger and Browne, 1984). The combination of variables with the first canonical coefficient for each set has the highest possible multiple correlations with the variables in the other set. CCA extracts canonical coefficients u and v such that $X_c = {x_c}^T u$ and $Y_c = {y_C}^T v$ (X_c and Y_c are canonical variates)

possess a maximum correlation coefficient (Chang et al., 2013) using the following function,

$$\begin{aligned} R &= \frac{E[X_c Y_c]}{sqrt(E[X_c^2]E[Y_c^2])} \\ &= \frac{E[u^T x_c {y_c}^T v]}{sqrt(E[u^T x_c {x_c}^T u]E[v^T y_c {y_c}^T v])} \\ &= \frac{u^T C_{x_c,y_c} v}{sqrt(u^T C_{x_c,x_c} u v^T C_{y_c,y_c} v])}, \end{aligned} \tag{8}$$

where C_{x_c,x_c} and C_{y_c,y_c} are covariance matrices of x_c and y_c, respectively and the objective in above function is to maximize the correlation R. We use an eigenvalue decomposition procedure to find the linear weights producing canonical coefficients, which imply maximum possible correlations (see details in Steiger and Browne, 1984). There are different canonical coefficients within each set leading to different uncorrelated coefficients. Nevertheless, the combination of variables with the first canonical coefficient for each set has the highest possible multiple correlations with the variables in the other set.

Two scenarios are considered for prediction: (i) the predictor (x_c) contains time series of both groundwater used for farming, industry, and human consumption from IWRMC and climate-related variables of precipitation, NDVI, and temperature (provided by Harris, 2008), and (ii) the predictor (x_c) includes only climate-related variables of precipitation, NDVI, and temperature. This is done to explore the impact of each scenario on water variations. The criterion (y_c) in both scenarios contains water storage (groundwater and soil moisture) and discharge (from IWRMC) variations. By applying CCA, we establish the best combinations between two sets of variables in two different cases. By comparing the results of these two scenarios, we can investigate how water use and climate variabilities impact water storage changes within Iran. Nevertheless, there are other effective components (e.g., large-scale ocean-atmosphere phenomenon, evaporation, and droughts) on the water storage, which is difficult to include all of them in the process. This CCA scheme, however, could provide an insight on the connection between the above components. Table 2 summarizes the experiments undertaken in this study. The corresponding research objectives and related sections that contain each experiment's results are also listed in the table.

TABLE 2

4. Results and discussion

4.1. Simulated assimilation

In the following, we analyze the effect of various scenarios of observations on the assimilation. As mentioned earlier, GRACE TWS observations are used to update the sum of soil moisture, vegetation, snow, and groundwater compartments at each grid cell. Thus, it is important to investigate the distribution of the increments between these compartments, especially soil moisture and groundwater storage while the influence of the remaining storages (i.e., vegetation and snow) is negligible. In particular, we are interested in monitoring the impacts of trends in observations time series on different water components. Schumacher et al. (2018) showed that assimilating GRACE TWS data can improve model simulation of seasonality and trend of TWS, as well as individual water storage components. This point is important because the largest part of GRACE TWS trends caused by groundwater variations that originate from both natural and human-induced (e.g. water use) changes while soil moisture variations generally follow climate pattern. Simulation experiments are undertaken to monitor how observations' variations, and particularly their trends are reflected in soil moisture and groundwater estimates during assimilation.

To illustrate how GRACE data assimilation can improve model states, we perform a synthetic study, in which arbitrary errors (uncertainty with different magnitudes) are assigned to different model derived water storage states. We evaluate whether these states accurately receive increments from GRACE TWS. To this end, we introduce different uncertainties to model states and test how these are transferred to the assimilation forecast steps (cf. Eqs. (3)-(4)). Figure 3 shows the relationship between selected uncertainties of water states and their corresponding weights in the (synthetic) assimilation. Based on this setup, six different scenarios are considered to explore the impact of weights as the ratio of the assigned increment derived for each storage state to the summation of all states. The results presented in Figure 3 indicate an average influence of assimilating GRACE TWS data into W3RA over Iran between 2003 and 2013. In general, as theoretically expected, higher weight (i.e., larger increment) is assigned to a variable with a smaller uncertainty. In other words, by assimilating GRACE TWS, the model's water states with larger uncertainty receive larger increments, and this is reverse for states with smaller uncertainty. These results approve the recent results of Schumacher et al. (2018), who assimilate GRACE TWS data into WGHM model over Australia. Figure 3 also shows that the average correlations between the individual estimated storage in each scenario

and the assimilated GRACE TWS. The correlations are calculated after removing seasonal effects on time series to focus on trends. It can be seen that larger correlations to the GRACE TWS trends are obtained for a compartment with larger uncertainty and correspondingly with a larger increment. This means that the assimilation process transfers the observation trends into the more uncertain storage, which receives the larger corrections.

FIGURE 3

Another synthetic experiment is also implemented, where, different observation sets are assimilated into W3RA but this time without manipulating their uncertainties. The aim is to investigate whether the distribution of increments of different water states changes when the TWS observations change. Here, four different synthetic observation scenarios are considered, which include two versions of the WaterGAP Global Hydrology Model (WGHM; more details on Döll et al., 2003; Müller et al., 2014) TWS estimates with and without water abstractions, GRACE-derived TWS, and GRACE TWS minus WGHM soil moisture that roughly gives groundwater observations. The spatially averaged time series of the TWS observations (for the first three cases) over Iran are displayed in Figure 4a. The difference between the WGHM TWS observations with and without water use clearly show the anthropogenic impacts as a distinct negative trend in WGHM with water abstraction impact. A similar trend can also be seen in GRACE TWS. Assimilation of these observations can show how water storages, for example their trends, are distributed between soil moisture and groundwater estimates. Assimilating WGHM TWS without water use, which does not show any significant trends, might better estimate soil moisture. This is due to the fact that the main source of TWS's negative trends is groundwater exploitation, while soil moisture variations generally are related to climatic (e.g., precipitation) variations. Hence, comparing the soil moisture results of assimilating GRACE TWS and WGHM TWS with water use with those of WGHM TWS without water use can help to assess the performance of data assimilation in updating soil moisture. Furthermore, while the first three observation sets (i.e., WGHM with and without water use and GRACE-derived TWS) are used to update the summation of all compartments, the last case (GRACE TWS minus WGHM soil moisture) is used to update only the groundwater simulations. The main rationale for updating only groundwater in the last experiment is to compare its results with the other scenarios, which can help to investigate how accurate groundwater corrections are

applied from TWS increments in the other cases, where different compartments are available.

FIGURE 4

The results of the data assimilation variants are shown in Figures 4b and 4c and updated groundwater estimates from assimilating GRACE TWS minus WGHM soil moisture is plotted in Figure 4c. The assimilation results for soil moisture (Figure 4b) and groundwater (Figure 4c) show that the negative TWS trends are largely reflected only in groundwater time series. The average correlation between the above TWS observations and corresponding groundwater estimates is 0.92, 42% (on average) larger than for the open-loop run, which indicates the suitability of data assimilation for constraining system states. For the entire area, there is a stronger agreement between the soil moisture from assimilation compared to the open-loop run, e.g., 22% (on average) for the GRACE TWS case and 28% (on average) for the WGHM TWS with water use case. Lower correlations are obtained for assimilating WGHM TWS without water use in comparison to other data assimilation scenarios (see also Figure 4b). Furthermore, groundwater variations from the assimilated GRACE TWS are largely correlated to the groundwater estimates from assimilating only groundwater observations (GRACE TWS minus WGHM soil moisture). TWS observations of WGHM without water use have the least effect on groundwater variations.

It can be concluded from Figure 4 that the data assimilation process successfully distributes TWS increments between soil moisture and groundwater storages. These results indicate that the largest part of increments during data assimilation is assigned to groundwater. The larger impact on groundwater, based on Figure 3, suggests that the groundwater estimation of W3RA is more uncertain than its soil moisture and as a result it receive larger updates. This is even more clear in Figure 5, where groundwater and soil moisture estimates by ensemble members between 2004 and 2008 are shown. This time period is selected because it includes an episode with strongly negative groundwater trend after 2005 (see also Figure 4c), where ensemble spreads show a different pattern, e.g., larger spreads. The propagated groundwater ensemble members are more dispersed than those of soil moisture, which causes larger ensemble deviations from its mean and consequently larger uncertainty for the states (cf. Eqs. (1)-(2)). This can be due to the point that the W3RA model has a simplified simulation of groundwater dynamics for unconfined groundwater and does not simulate confined groundwater dynamics or anthropogenic

groundwater extraction (Tregoning et al., 2012). The larger corrections applied to groundwater is also realistic considering the fact that a majority of water depletion in Iran occurs in groundwater due to large extractions for irrigation. The applied irrigation water is likely to locally increase total soil column water storage, which may contribute to a smaller decline in soil water content (Michel, 2017).

FIGURE 5

Even though the results indicate good performance of GRACE data assimilation, one might still expect artefacts from the TWS increments on the state estimates. The absence of groundwater abstractions and anthropogenic impacts in most hydrological models, especially where the rate of this extraction is high, can cause a misinterpretation of a negative TWS trend captured by GRACE in the system states. As shown by Girotto et al. (2017), the assimilation of GRACE TWS can successfully introduce the negative trends in the modeled TWS and groundwater, however, this can also introduce unrealistic decline in other components, e.g., soil moisture and evapotranspiration. This effect can be exacerbated when groundwater extraction is large and occurs over an extended period. The model dynamical range of groundwater may not be sufficient to accommodate the assimilated values (Zaitchik et al., 2008; Li and Rodell, 2015). Despite these, merging GRACE TWS data with high resolution models is the most efficient existing approach to analyze groundwater changes over wide areas, which in most cases results in an improvement in the estimates (Li and Rodell, 2015; Girotto et al., 2017). Here, we addressed this challenge by conducting a synthetic experiment, as well as by independently assessing groundwater and soil moisture from assimilation. However, more investigations are needed to be extended and the impacts of various data assimilation scenarios on each individual water compartments need to be tested. These investigations are, however, out of the scope of this study.

4.2. Result evaluation

In this section, we assess the performance of data assimilation using in-situ groundwater measurements. To examine the validity of data assimilation results, in-situ groundwater measurements of the six major drainage regions in the area including the East, Caspian Sea, Centre, Sarakhs, Persian Gulf and Oman Sea, and Lake Urmia (cf. Figure 1) are used. For each basin in Figure 1, we calculate the spatial average time series of groundwater storages with and without

data assimilation and compare them with the IWRMC in-situ and WGHM groundwater variation. We first analyze the performance of two assimilation cases of GRACE TWS and GRACE TWS minus WGHM soil moisture data assimilation experiments for improving groundwater estimates. Figure 6 shows the average root-mean-square error (RMSE) and standard deviation (STD) calculated using groundwater from assimilation cases and in-situ measurements. Both cases perform comparably in terms of RMSE and STD with an average of 38% error reduction compared to open-loop. Nevertheless, assimilating GRACE TWS obtains the smaller RMSE than groundwater only data assimilation. This further confirms the effectiveness of the applied data assimilation for distribution TWS increments, especially for groundwater storage. Based on this assessment, hereafter only the results for GRACE TWS data assimilation are presented.

FIGURE 6

The results for groundwater examination from data assimilation, WGHM, and the open-loop run for each drainage division are illustrated in Figure 7, which show that the strongest agreement between groundwater estimates and in-situ measurements occur in the assimilation results. In most of the cases, WGHM performs better than the open-loop. For a better assessment of data assimilation results, additional agreement statistics using RMSE and correlation analysis are calculated and reported in Table 3. Significance at $p < 0.05$ was calculated using the Students t-test with consideration of temporal autocorrelation through effective sample size.

FIGURE 7

TABLE 3

The computed time series for each region is compared to IWRMC data for the corresponding region in order to estimate the reported statistics in Table 3. Generally, the assimilation results are largely correlated with the in-situ data (0.85 on average) after data assimilation, with an improvement of 35% over open-loop results. The largest improvements in terms of correlation increase and RMSE reduction with respect to the in-situ measurements are achieved over Lake Urmia, Sarakhs, and to a lesser degree Persian Gulf and Oman Sea. Table 3 shows considerable groundwater decline in most of the regions especially within the Persian Gulf and Oman Sea and Lake Urmia (both mostly located in the western areas). The largest negative groundwater

trend is exhibited for Lake Urmia while the lowest trend is found for the Caspian Sea division in the north, which could be attributed to a large amount of precipitation in the latter region.

We further examine the soil moisture estimates from data assimilation. In the absence of reliable in-situ soil moisture measurements over the study area, we use satellite-derived and independent model soil moisture products. Soil moisture observations from the Advanced Microwave Scanning Radiometer - Earth Observing System (AMSR-E) and Soil Moisture and Ocean Salinity (SMOS) are compared to the assimilated top layer soil moisture estimates. The motivation behind this comparison is based on the fact that SMOS and AMSR-E measurements are largely correlated, respectively, to surface 0-5 cm and 0-2 cm soil moisture content (Njoku et al., 2003). Figure 8 shows the average time series of the above comparison within the study period. It can be seen that the assimilation top layer soil moisture is better matched (41% improvement in correlation) to the satellite measurements in comparison to the open-loop estimates. This shows a successful impact of GRACE TWS data assimilation on the model top layer.

FIGURE 8

Total soil moisture estimates from data assimilation, i.e., summation of soil moisture at top, shallow- and deep-root layers, are compared with soil moisture estimates of WGHM, the Global Land Data Assimilation System (GLDAS; Rodell et al., 2004), and soil moisture provided by van Dijk et al. (2014), who combined different data (e.g., GRACE) and model outputs (indicated here as W3). The results are displayed in Figure 9. In all cases, data assimilation leads to a better agreement to other products with an average 25% improvement. The largest correlation, as well as the greatest improvement, are found for soil moisture after assimilation of WGHM. There is also a considerable correlation between the results and W3.

FIGURE 9

4.3. Water storage analysis

Based on the improved soil moisture and groundwater estimates, spatio-temporal variations of both compartments are analyzed in this section. The variation of groundwater storages within Iran before and after data assimilation are illustrated in Figure 10. The blue graph in Figure 10 represents the average groundwater variations of all grid points after data assimila-

tion. This graph clearly shows a negative trend between 2002 and 2013 with an average -8.9 mm/year groundwater depletion for the entire country. However, such a trend is not present in the open-loop time series. GRACE TWS data assimilation constrains groundwater estimates and introduces this negative trend into the state as it exists in GRACE TWS observations (cf. Figure 4). It is evident that the W3RA without data assimilation is not able to provide reliable long-term changes of groundwater, e.g., trend and multi-year variations. Therefore, data assimilation is vital for reliable interpretation of ground water beyond the annual cycle. However, without additional information the data assimilation results cannot differentiate between natural and anthropogenic causes. Apart from the trends, Figure 10 also shows a multi-year cycle, e.g., positive trend between 2002 and 2005 and a stronger negative trend for the later years 2006 to 2013. Again, this trend is not visible in the open-loop simulations.

FIGURE 10

Furthermore, we separately analyze water compartments for each of Iran's major drainage regions. The soil moisture and groundwater average time series from W3RA before and after assimilating GRACE TWS for each of the divisions are shown in Figure 11 and Figure 12, respectively. Larger soil moisture variations (in terms of amplitude) exist for the data assimilation results compared to open-loop results in Figure 11. In particular, this is evident for the Persian Gulf and Oman Sea and Caspian Sea. This could be due to a larger amount of annual precipitation over these areas. Declines in soil water content can be seen in Sarakhs, especially between 2005 and 2009, and Lake Urmia. In most of the regions, increases (e.g., large positive variations) are observed during 2004 and 2010. Overall, better agreements between open-loop and assimilation time series are found over East and Centre regions, where a semi-arid climate condition is dominant. GRACE data assimilation has the least impact on soil moisture estimates within these areas.

FIGURE 11

Figure 12 depicts groundwater variations for each individual drainage division. Similar to soil moisture analysis (cf. Figure 11), data assimilation results demonstrate larger magnitudes than open-loop results. Except for the Caspian Sea, all the regions show a considerable decline in groundwater estimates during the study period. In particular, this is clear in Lake Urmia,

Sarakhs, and Centre, especially after 2007. These trends are absent in the open-loop time series and derive from GRACE TWS after implementing data assimilation, which confirm the results shown in Figure 10. Larger groundwater declines are found in regions over the western parts of the country (e.g., the Persian Gulf and Oman Sea and Lake Urmia). In most of the cases, groundwater rise is observed as a positive trend between 2004 and 2005. These increases are then followed by consistent declines despite some short-term increases such as during 2010. A large trend decline is observed after 2006 in Lake Urmia, Centre, Sarakhs, and to a lesser degree in Caspian Sea. For the Persian Gulf and Oman Sea, Sarakhs, and Center, the groundwater negative trend is remarkable after 2008. Despite a small negative trend in East for the study period, the groundwater variations have the smallest amplitudes in this region compared to other areas. Seasonal variations can clearly be seen in most of the regions while this pattern is dominant mostly in Caspian Sea. Figure 12 and the reported negative trends in Table 3 show that groundwater depletion is a major issue in most parts of Iran resulting in a remarkable dryness across the country.

FIGURE 12

4.4. Climatic impacts

We further investigate the connection between climatic impacts and water storage variations. A comparison between groundwater and soil moisture variations and climate-related variables such as precipitation and NDVI can reveal such interactions these parameters. Figure 13 shows maps of temporal average precipitation, soil moisture, and groundwater maps during the study period. The first row in Figure 13 represent the average applied increment to soil moisture and groundwater storages, the second row indicates variations (average of time series at each grid point) of precipitation, soil moisture, and groundwater, and trends for each variable at each grid point are depicted in the third row.

FIGURE 13

Figure 13 shows the spatial pattern of increments, i.e., the difference between assimilation results and open-loop estimates, applied to the system states. It can be seen that the largest increments are applied to groundwater storage as can be expected from Figures 3 and 4. These corrections are mostly focused on the northwest to south and the eastern part of Iran. In soil

moisture, the increments can be found across the country, again, with larger concentrations in the western areas. The effect of data assimilation clearly can be seen by the increments illustrated in Figure 13. The spatial pattern of precipitation, soil moisture, and groundwater variations in Figure 13 show larger variations over the north toward northwest parts, where the Alborz mountain range cover a large portion of the areas. A similar pattern can also be seen in western parts, where the Zagros mountain range is located. Overall, the soil moisture map more closely reflects the precipitation patterns compared to groundwater variations, which can be attributed to impacts from water uses. Contrary to precipitation and soil moisture, negative groundwater variations are found over different regions, especially the north-western and southern parts. There are very limited variations in terms of amplitude changes for precipitation, soil moisture, and groundwater within the centre, eastern, and partially south-eastern parts of Iran. Trend maps (last row in Figure 13) illustrate spatial patterns for each component. Both precipitation and soil moisture show increasing trends in the north and to a lesser degree in the south. Groundwater trends are generally negative in all regions, but more strongly in the west, where Lake Urmia is located. A significant groundwater depletion can be observed in the central parts extended to the north, where Tehran, Iran's capital city is located. Large groundwater extractions in Tehran during the study period can be the main reason for this while in other areas, an excessive irrigation is a potential candidate for the observed depletion. It can be seen that there is an agreement between the applied increment by data assimilation, especially for groundwater, and the negative observed trends. Again it can be concluded that without using assimilation, these negative trends are not captured.

To better quantify the spatio-temporal variations of water storage and climate variabilities, principal component analysis (PCA Lorenz, 1956) is applied on precipitation, NDVI, GRACE TWS, and groundwater time series. This allows us to monitor the relationship between the estimated groundwater and GRACE TWS, as well as their connection to climatic impacts through precipitation and NDVI. The first three extracted principal components (PC1, PC2, and PC3) of each component are plotted in Figure 14. There is good agreement between the time series for all three cases, in particular for seasonal variations. All time series in PC1 show a clear annual variation. Negative trends, especially after 2009 are only captured by PC1 of GRACE TWS and groundwater. Stronger agreements between precipitation and NDVI PCs can be found. This can be attributed to vegetation growth response to rainfall and soil moisture. The assimilated groundwater storage variations largely follow the GRACE TWS

variation patterns, both in terms of variability and trend, mainly due to the application of GRACE data assimilation. Both of these variables are strongly correlated with rainfall time series in PC2 and PC3 with an average correlation of 0.86. Various strong anomalies are occur in the time series, e.g., in 2005 and 2010. Increases in the time series occur in PC1 for all variables between 2004 and 2006 and during 2010 and 2012. PC2 shows similar rises in 2008 and 2010 followed by a strong decrease. PC3 shows an increase in 2009 and 2010 in the precipitation, GRACE TWS, and groundwater which explains the corresponding increase in water storages (cf. Figures 10 and 12). Some negative anomalies are found in PC3 in 2003, 2005, and 2011 and also in 2006 and 2013. The other variables generally demonstrate the same variation pattern as precipitation, which shows a strong connection between water storage variations and climatic changes. Water storage variations in Iran, however, are also affected by non-climate factors (e.g., anthropogenic impacts), which are likely the cause of the observed negative trends in PC1 for GRACE TWS and groundwater.

FIGURE 14

The corresponding empirical orthogonal functions (EOF1, EOF2, and EOF3) extracted by applying PCA on precipitation, NDVI, GRACE TWS, and groundwater from data assimilation are shown in Figure 15. Overall, the mode 1 represents a strong annual signal (as would be expected), mode 2 shows some deviations from the annual signal (e.g. inter-annual variations) in the same regions as for mode 1. Mode 3 to some extent shows inter-annual variations but importantly shows some extreme values. The spatial patterns of NDVI, GRACE TWS, and groundwater are largely correlated to rainfall pattern, especially in EOF1 and EOF2. Larger spatial variations exist over the northern and western parts of Iran, which seem to cause larger water storage and NDVI changes in the same areas. These are the parts with higher altitudes in which precipitation rates are generally high. GRACE TWS and groundwater EOF2 maps show strong positive signals over the north toward the northwest and partially in western areas. The rainfall EOF2 map, however, does not show a large signal over the north-western part but only over the northern and western parts, where the Alborz and Zagros mountain ranges are located. On the other hand, all variables show a negative signal in the south-eastern part. Positive signals over the eastern parts, with smaller amplitudes, compared to EOF1 and EOF2 for NDVI, GRACE TWS, and groundwater are displayed by EOF3 maps. Negative signals can

be seen in EOF3 maps, especially for groundwater mostly over the northwestern areas, where Lake Urmia is located, as well as the northeast and Sarakh.

FIGURE 15

4.5. CCA results

We further implement CCA on the estimated water compartments (from the data assimilation) on the one hand, and human- as well as climate-related variables on the other hand in two different scenarios, i.e., (i) the predictor contains time series of both groundwater used (e.g., for farming and industry) and climate-related variables (precipitation, NDVI, and temperature), and (ii) the predictor includes only climate-related variables of precipitation, NDVI, and temperature (cf. Section 3.2). By this, we can establish the relations between water storages and other factors. CCA is applied to the spatially averaged time series of all variables to estimate canonical coefficients. Canonical loadings are used to interpret the CCA results, which measure the simple linear correlation between an observed variable and the estimated canonical variates (Dattalo, 2014). The interpretation is mostly based on examining the sign and the magnitude of the canonical coefficients assigned to each variable. Variables with larger coefficients contribute more to the variates and variables with opposite signs exhibit an inverse relationship with each other while those with the same sign exhibit a direct relationship. Detailed results of the CCA experiment for each scenario applied within Iran are presented in Table 4.

TABLE 4

The table summarizes the contribution of each variable in CCA. Results indicate that scenario (i) leads to larger canonical correlation coefficients in comparison to scenario (ii). This means that variations in water storages are more correlated to variations of the combined human- and climate-related parameters. Note that CCA extract different sets of results (roots), thus, we only use the first root that is statistically significant (for a significant level of 0.05). It can be seen from Table 4 that the water use has strong negative correlations to water storage variations, especially groundwater, which has the largest loading. This means that water consumption for various uses (especially farming) is a very effective factor within the country that causes the greatest impact on groundwater (with 0.938 canonical correlation). Among climate

variables, precipitation, and to a lesser degree temperature have also a considerable influence on water storage variations. Not surprisingly, an increase (or decrease) in rainfall directly leads to increase (or decrease) in water storages as indicated by the same signs. Table 4 suggests that variations in groundwater use and climate parameters in both scenarios have minimum impact on water discharge. This may be due to the fact that surface waters compose a relatively small amount of water availability across Iran in comparison to other storages such as groundwater.

It can also be inferred from Table 4 that removing the water use from scenario (i) results in smaller canonical correlation in (ii), which means a smaller agreement between variables in scenario (ii) and water storage changes, even though this removal causes ∼3% and 5% increase in loadings of precipitation and temperature, respectively. Comparing the results of both scenarios implies the large anthropogenic impact (more than climate-related factors) on water storages variations, which makes it essential to include this impact along with climatic effects while one studies sub-surface water storage variations in Iran. Figure 16 depicts scatter bi-plots and the linear trend which represents the correspondence between two sets of variables using average canonical coefficients for each scenario. It can be seen that the distribution of the two datasets in scenario (i) has smaller deviations and is more symmetric (closer to the reference line than scenario (ii)), which leads to higher canonical correlation for the first scenario. Figure 16 shows that incorporating the water use results in a better agreement between the criterion, i.e., water storage variations and predicant. This stresses the necessity of considering the water use and anthropogenic impacts (e.g., irrigation) on water storages analyzes, which cannot be happen without inclusion of GRACE TWS into the process.

FIGURE 16

5. Conclusions

Sub-surface water storages are a major source of freshwater in Iran. With increased population and irrigated land, water availability has become a serious issue across the country. In the present study we assimilate GRACE TWS into W3RA to separately analyze different water compartments including groundwater, soil moisture, and surface water storages. The six major drainage divisions in the area including the eastern part of Iran (East), Caspian Sea, Centre, Sarakhs, Persian Gulf and Oman Sea, and Lake Urmia are considered to better understand water availability in the different regions. An analysis is undertaken to examine the

effects of GRACE data assimilation on different water storage compartments. It is found that the implemented process can effectively distribute the TWS increments between groundwater and soil moisture storages. Although the results show improvements in both groundwater and soil moisture, the data assimilation still may have introduced some artefacts into the simulated groundwater dynamics due to the massive effects of groundwater extraction within the country, which requires an independent extensive study and more comprehensive analysis.

It is found that the application of GRACE TWS data assimilation can significantly improve the performance of W3RA. Data assimilation successfully correct for the open-loop simulation variations, e.g., in terms of trends and multi-year variations, especially for groundwater storage. Based on the improved estimates, we find that groundwater trends in a large part of the country's central, western and southern areas are negative representing a significant water availability issue. An average -8.9 mm/year water storages decline is observed during 2002 to 2012 with a larger rate since 2005 suggesting that Iran is becoming considerably dryer. Larger water store depletions are found to occur in the Persian Gulf and Oman Sea and Lake Urmia with lesser effects on soil moisture in these regions. In the Caspian Sea region, however, due to a large amount of precipitation, smaller groundwater and soil moisture trends are observed. In the Persian Gulf and Oman Sea, -9.3 mm/year (on average) groundwater trend is found, which is the second largest negative trend after that of Lake Urmia.

Furthermore, PCA is applied to investigate the relationship between the estimated groundwater and GRACE TWS, as well as their connection to climatic impacts in various parts of Iran. Larger water storage spatial variations are observed over the northern and western parts of Iran with higher altitudes in which precipitation rates are generally high. Contrary to rainfall maps, strong positive GRACE TWS and groundwater signals are found over the north toward the northwest and partially in western areas. In terms of temporal variations, water storage variables generally demonstrate the same variation pattern as precipitation, however, they are also affected by non-climate factors (e.g., anthropogenic impacts), which are likely the cause of the observed negative trends in GRACE TWS and groundwater time series. Therefore, CCA is applied to explore the relationship between water storages estimated by data assimilation and climatic, as well as anthropogenic indicators. The application of CCA reveals strong correlation (0.89 in average) suggesting that the groundwater use has a major impact on water storage variations.

Acknowledgement

M. Khaki is grateful for the research grant of Curtin International Postgraduate Research Scholarships (CIPRS)/ORD Scholarship provided by Curtin University (Australia). This work is a TIGeR publication.

References

Afshar, A.A., Joodaki, G.R., Sharifi, M.A. (2016). Evaluation of Groundwater Resources in Iran Using GRACE Gravity Satellite Data. JGST., 5 (4) :73-84, http://jgst.issge.ir/article-1-381-fa.html.

Amery, H.A., Wolf, A.T. (2000). Water in the Middle East: A Geography of Peace, University of Texas Press, Austin, Tex.

AAnderson, J. (2001). An Ensemble Adjustment Kalman Filter for Data Assimilation. Mon. Wea. Rev., 129, 28842903, http://dx.doi.org/10.1175/1520-0493(2001)129¡2884:AEAKFF¿2.0.CO;2.

Anderson, M.C., Norman, J.M., Mecikalski, J.R., Otkin, J.A., Kustas, W.P. (2007). A climatological study of evapotranspiration and moisture stress across the continental United States based on thermal remote sensing: 1. Model formulation. J. Geophys. Res. 112 (D10117). http://dx.doi.org/10.1029/2006JD007506.

Ardakani, R. (2009). Overview of water management in Iran. Proceeding of regional center on urban water management, Tehran, Iran.

Bennett, A.F. (2002); Inverse Modeling of the Ocean and Atmosphere, 234 pp., Cambridge Univ. Press, New York.

Bertino, L., Evensen G., Wackernagel, H. (2003). Sequential Data Assimilation Techniques in Oceanography, International Statistical Review, Vol. 71, No. 2, pp. 223-241.

Chang, B., Kruger, U., Kustra, R., Zhang, J. (2013). Canonical Correlation Analysis based on Hilbert-Schmidt Independence Criterion and Centered Kernel Target Alignment, Volume 28: Proceedings of The 30th International Conference on Machine Learning, 2, 28, 316-324, http://jmlr.csail.mit.edu/proceedings/papers/v28/chang13.pdf.

Chen, J.L., Wilson, C.R., Famiglietti, J.S., Rodell, M. (2007). Attenuation effect on seasonal basin-scale water storage changes from GRACE time-variable gravity. Journal of Geodesy, 81, 4, 237245. http://dx.doi.org/10.1007/s00190-006-0104-2.

Chen, J.L., Wilson, C.R., Tapley, B.D. (2013). Contribution of ice sheet and mountain glacier melt to recent sea level rise. Nat. Geosci., 6, 549552, http://dx.doi.org/10.1038/ngeo1829.

Cheng, M.K., Tapley, B.D. (2004). Variations in the Earth's oblateness during the past 28 years. Journal of Geophysical Research, Solid Earth, 109, B09402. http://dx.doi.org/10.1029/2004JB003028.

Coumou, D., Rahmstorf, S. (2012). A decade of weather extremes Nat. Clim. Change, 2 (7), pp. 16.

Dattalo, P. (2014). A demonstration of canonical correlation analysis with orthogonal rotation to facilitate interpretation. Unpublished manuscript, School of Social Work, Virginia Commonwealth University, Richmond, Virginia.

Döll, P., Kaspar, F., Lehner, B. (2003). A global hydrological model for deriving water availability indicators: model tuning and validation, J. Hydrol., 270, 105134.

Eicker, A., Schumacher, M., Kusche, J., Dll, P., Mller-Schmied, H., (2014). Calibration/data assimilation approach for integrating GRACE data into the WaterGAP global hydrology model (WGHM) using an ensemble Kalman filter: first results, SurvGeophys, 35(6):12851309. http://dx.doi.org/10.1007/s10712-014-9309-8.

Evensen, G. (2003). The ensemble Kalman filter: Theoretical formulation and practical inplementation, Ocean Dynamics, 53, 343367, http://dx.doi.org/10.1007/s10236-003-0036-9.

FAO (Food and Agriculture Organization of the United Nations)(2009). FAO water report, 34.

Fatolazadeh, F., Voosoghi, B., Naeeni, M.R. (2016). Wavelet and Gaussian Approaches for Estimation of Groundwater Variations Using GRACE Data. Groundwater, 54: 7481, http://dx.doi.org/10.1111/gwat.12325.

Forootan, E., Rietbroek, R., Kusche, J., Sharifi, M.A., Awange, J., Schmidt, M., Omondi, P., Famiglietti, J. (2014a). Separation of large scale water storage patterns over Iran using

GRACE, altimetry and hydrological data. Journal of Remote Sensing of Environment, 140, 580-595, http://doi.org/10.1016/j.rse.2013.09.025.

Forootan, E., Didova, O., Schumacher, M., Kusche, J., Elsaka, B. (2014b). Comparisons of atmospheric mass variations derived from ECMWF reanalysis and operational fields, over 2003 to 2011. Journal of Geodesy, 88, Pages 503-514, http://dx.doi.org/10.1007/s00190-014-0696-x.

Forootan, E., Safari, A., Mostafaie, A., Schumacher, M., Delavar, M., Awange, J. (2017). Large-scale total water storage and water flux changes over the arid and semi-arid parts of the Middle East from GRACE and reanalysis products. Surveys in Geophysics, http://dx.doi.org/10.1007/s10712-016-9403-1.

Garner, T.W., Wolf, R.A., Spiro, R.W. , Thomsen, M.F. (1999). First attempt at assimilating data to constrain a magnetospheric model, J. Geophys. Res., 104(A11), 2514525152, http://dx.doi.org/10.1029/1999JA900274.

Girotto, M., De Lannoy, G.J., Reichle, R.H., Rodell, M. (2016). Assimilation of gridded terrestrial water storage observations from GRACE into a land surface model. Water Resources Research, 52(5), 4164-4183.

Girotto, M., De Lannoy, G.J., Reichle, R.H., Rodell, M., Draper, C., Bhanja, S.N., Mukherjee, A. (2017). Benefits and Pitfalls of GRACE Data Assimilation: a Case Study of Terrestrial Water Storage Depletion in India. Geophysical Research Letters.

Golian, S., Mazdiyasni, O., AghaKouchak, A. (2015). Trends in meteorological and agricultural droughts in Iran. Theor Appl Climatol (2015) 119:679688, http://dx.doi.org/10.1007/s00704-014-1139-6.

Harris, I.C. (2008). Climatic Research Unit (CRU) time-series datasets of variations in climate with variations in other phenomena. NCAS British Atmospheric Data Centre, date of citation, University of East Anglia Climatic Research Unit; Jones, P.D., http://catalogue.ceda.ac.uk/uuid/3f8944800cc48e1cbc29a5ee12d8542d.

Hoteit, I., Pham, D.T., Triantafyllou, G., Korres, G. (2008). A new approximate solution of the optimal nonlinear filter for data assimilation in meteorology and oceanography, Monthly Weather Review, 136, 317-334.

Hoteit, I., Pham, D.T., Gharamti, M. E., Luo, X. (2015). Mitigating Observation Perturbation Sampling Errors in the Stochastic EnKF, Monthly Weather Review, 143:7, 2918-2936.

Huntington, T.G. (2006). Evidence for intensification of the global water cycle: Review and synthesis, J. Hydrol.,319(14), 8395, http://dx.doi.org/10.1016/j.jhydrol.2005.07.003.

Joodaki, G., Wahr, J., Swenson, S. (2014). Estimating the human contribution to groundwater depletion in the Middle East, from GRACE data, land surface models, and well observations, Water Resour. Res., 50, 26792692, http://dx.doi.org/10.1002/2013WR014633.

Kalnay, E. (2003). Atmospheric modelling, data assimilation and predictability. Cambridge University Press. pp. xxii 341. ISBNs 0 521 79179 0, 0 521 79629 6, http://dx.doi.org/10.1256/00359000360683511.

Karamouzian, M., Haghdoost, A.K. (2015). Population control policies in Iran, The Lancet, Volume 385, Issue 9973, 2127 March 2015, Page 1071, ISSN 0140-6736, https://doi.org/10.1016/S0140-6736(15)60596-7.

Khaki, M., Forootan, E., Sharifi, M.A. (2014). Satellite radar altimetry waveform retracking over the Caspian Sea. Int. J. Remote Sens., 35(17), 63296356, http://dx.doi.org/10.1080/01431161.2014.951741.

Khaki, M., Forootan, E., Sharifi, M.A., Awange, J., Kuhn, M., (2015). Improved gravity anomaly fields from retracked multimission satellite radar altimetry observations over the Persian Gulf and the Caspian Sea. Geophys. J. Int. 202 (3): 1522-1534, http://dx.doi.org/10.1093/gji/ggv240.

Khaki, M., Hoteit, I., Kuhn, M., Awange, J., Forootan, E., van Dijk, A.I.J.M., Schumacher, M., Pattiaratchi, C., (2017a). Assessing sequential data assimilation techniques for integrating GRACE data into a hydrological model, Advances in Water Resources, Volume 107, Pages 301-316, ISSN 0309-1708, http://dx.doi.org/10.1016/j.advwatres.2017.07.001.

Khaki, M., Ait-El-Fquih, B., Hoteit, I., Forootan, E., Awange, J., Kuhn, M., (2017b). A Two-update Ensemble Kalman Filter for Land Hydrological Data Assimilation with an Uncertain Constraint, Journal of Hydrology, Available online 25 October 2017, ISSN 0022-1694, https://doi.org/10.1016/j.jhydrol.2017.10.032.

Khaki, M., Schumacher, M., J., Forootan, Kuhn, M., Awange, E., van Dijk, A.I.J.M., (2017c). Accounting for Spatial Correlation Errors in the Assimilation of GRACE into Hydrological Models through localization, Advances in Water Resources, Available online 1 August 2017, ISSN 0309-1708, https://doi.org/10.1016/j.advwatres.2017.07.024.

Khaki, M., Forootan, E., Kuhn, M., Awange, J., Papa, F., Shum, C.K., (2018a). A Study of Bangladesh's Sub-surface Water Storages Using Satellite Products and Data Assimilation Scheme, Science of The Total Environment, Volume 625, 2018, Pages 963-977, ISSN 0048-9697, https://doi.org/10.1016/j.scitotenv.2017.12.289.

Khaki, M., Forootan, E., Kuhn, M., Awange, J., Longuevergne, L., Wada, W., (2018b). Efficient Basin Scale Filtering of GRACE Satellite Products, In Remote Sensing of Environment, Volume 204, Pages 76-93, ISSN 0034-4257, https://doi.org/10.1016/j.rse.2017.10.040.

Knapp, T.R. (1978). Canonical correlation analysis: A general parametric significance-testing system. Psychological Bulletin. 85 (2): 410416. http://dx.doi.org/10.1037/0033-2909.85.2.410

Kusche, J., Schmidt R., Petrovic, S., Rietbroek, R. (2009). Decorrelated GRACE time-variable gravity solutions by GFZ and their validation using a hydrological model, Journal of Geodesy, DOI 10.1007/s00190-009-0308-3.

Lahoz, W.A., Geer, A.J., Bekki, S., Bormann, N., Ceccherini, S., Elbern, H., Errera, Q., Eskes, H.J., Fonteyn, D., Jackson, D.R., Khattatov, B. (2007). The Assimilation of Envisat data (ASSET) project, Atmos. Chem. Phys., 7, 1773 - 1796.

Li, B., Rodell, M. (2015). Evaluation of a model-based groundwater drought indicator in the conterminous US. Journal of Hydrology, 526, 78-88.

Lorenz, E. (1956). Empirical orthogonal function and statistical weather prediction. Technical Report Science Report No 1, Statistical Forecasting Project. MIT, Cambridge.

Madani, K. (2014). Water management in Iran: what is causing the looming crisis? J Environ Stud Sci. doi:10.1007/s13412-014-0182-z.

Mayer-Gürr, T., Zehentner, N., Klinger, B., Kvas, A. (2014). ITSG-Grace2014: a new GRACE gravity field release computed in Graz. - in: GRACE Science Team Meeting (GSTM), Potsdam am: 29.09.2014.

Michel, D. (2017). Iran's impending water crisis. In Water, Security, and US Policy, edited by David Reed. 438 pages, ISBN-10:1138051519.

Mohammadi-Ghaleni, M., Ebrahimi, K. (2011). Assessing impact of irrigation and drainage network on surface and groundwater resources Case study: Saveh Plain, Iran, ICID 21st International Congress on Irrigation and Drainage, 1523 October 2011, Tehran, Iran.

Motagh, M., Walter, T.R., Sharifi, M.A., Fielding, E., Schenk, A., Anderssohn, J., et al. (2008). Land subsidence in Iran caused by widespread water reservoir overexploitation. Geophysical Research Letters, 35, L16403. http://dx.doi.org/10.1029/2008GL033814.

Müller Schmied, H., S. Eisner, D. Franz, M. Wattenbach, F. Portmann, M. Flrke, and P. Dll (2014), Sensitivity of simulated global-scale freshwater fluxes and storages to input data, hydrological model structure, human water use and calibration, Hydrol. Earth. Syst. Sci., 18, 35113538, http://dx.doi.org/10.5194/hess-18-3511-2014.

Munier, S., Aires, F., Schlaffe, S., Prigent, C., Papa, F., Maisongrande, P., Pan, M. (2014). Combining data sets of satellite-retrieved products for basin-scale water balance study: 2. Evaluation on the Mississippi Basin and closure correction model. Journal of Geophysical Research: Atmospheres, 119, 12,100-12,116, http://dx.doi.org/10.1002/2014JD021953.

Njoku, E.G. et al. (2003). Soil moisture retreival from AMSR-e. IEEE Transactions on Geoscience and Remote Sensing. 41:2, 215-229.

Ott, E., Hunt, B.R., Szunyogh, I., Zimin, A.V., Kostelich, E.J., Corazza, M., Kalnay, E., Patil, D.J., Yorke, J.A. (2004). A local ensemble Kalman Filter for atmospheric data assimilation. Tellus, 56A: 415-428.

Oke, P.R., Brassington, G.B., Griffin, D.A., Schiller, A. (2008). The Bluelink Ocean Data Assimilation System (BODAS). Ocean Modelling, 21, 4670, http://dx.doi.org/10.1016/j.ocemod.2007.11.002.

Reager, J.T., Thomas, A.C., Sproles, E.A., Rodell, M., Beaudoing, H.K., Li, B., Famiglietti, J.S. (2015). Assimilation of GRACE Terrestrial Water Storage Observations into a Land Surface Model for the Assessment of Regional Flood Potential. Remote Sens. 2015, 7, 14663-14679.

Renzullo, L.J., Van Dijk, A.I.J.M., Perraud, J.M., Collins, D., Henderson, B., Jin, H., Smith, A.B., McJannet, D.L. (2014). Continental satellite soil moisture data assimilation improves

root-zone moisture analysis for water resources assessment. J. Hydrol., 519, 27472762. http://dx.doi.org/10.1016/j.jhydrol.2014.08.008.

Rodell, M., Houser, P. R., Jambor, U., Gottschalck, J., Mitchell, K., Meng, C. J., Arsenault, K., Cosgrove, B., Radakovich, J., Bosilovich, M., Entin, J. K., Walker, J. P., Lohmann, D., Toll, D. (2004). The global land data assimilation system. American Meteorological Society, 85, 3, 381-394. http://dx.doi.org/10.1175/BAMS-85-3-381.

Sarraf, M., Owaygen, M., Ruta, G., Croitoru, L. (2005). Islamic Republic of Iran: Cost assessment of environmental degradation. Tech. Rep. 32043-IR. Washington, D.C.: World Bank.

Schmidt, R., Petrovic, S., Gntner, A., Barthelmes, F., Wnsch, J., Kusche, J. (2008). Periodic components of water storage changes from GRACE and global hydrology models. J. Geophys. Res., 113, B08419, http://dx.doi.org/10.1029/2007JB005363.

Schumacher, M., Kusche, J., Döll, P. (2016). A systematic impact assessment of GRACE error correlation on data assimilation in hydrological models, Journal of Geodesy, http://dx.doi.org/10.1007/s00190-016-0892-y.

Schumacher, M., Forootan, E., van Dijk, A.I.J.M., Mller Schmied, H., Crosbie, R.S., Kusche, J., Dll, P. (2018). Improving drought simulations within the Murray-Darling Basin by combined calibration/assimilation of GRACE data into the WaterGAP Global Hydrology Model, Remote Sensing of Environment, Volume 204, 2018, Pages 212-228, ISSN 0034-4257, https://doi.org/10.1016/j.rse.2017.10.029.

Schunk, R.W., Scherliess, L., Sojka, J.J., Thompson, D.C. (2004). USU global ionospheric data assimilation models, Atmospheric and Environmental Remote Sensing Data Processing and Utilization: an End-to-End System Perspective, (ed. H.-L. A. Huang and H. J. Bloom), Proc. of SPIE, 5548, http://dx.doi.org/10.1117/12.562448, 327-336.

Sheffield, J., Goteti, G., Wood, E.F. (2006). Development of a 50-yearhigh-resolution global dataset of meteorological forcings for land surfacemodeling, J. Clim., 19(13), 30883111.

Steiger, J.H., Browne, M.W. (1984). The comparison of interdependent correlations between optimal linear composites. Psychometrika, 49, 1121.

Stewart, L.M., Dance, S.L., Nichols, N.K. (2008). Correlated observation errors in data assimilation. Int. J. Numer. Meth. Fluids, 56: 15211527. http://dx.doi.org/10.1002/fld.1636.

Swenson, S., Chambers, D., Wahr, J. (2008). Estimating geocentervariations from a combination of GRACE and ocean model output. Journal of Geophysical research, 113, B08410, http://dx.doi.org/10.1029/2007JB005338.

Tangdamrongsub, N., Steele-Dunne, S.C., Gunter, B.C., Ditmar, P.G., and Weerts, A.H. (2015). Data assimilation of GRACE terrestrial water storage estimates into a regional hydrological model of the Rhine River basin, Hydrol. Earth Syst. Sci., 19, 2079-2100, http://dx.doi.org/10.5194/hess-19-2079-2015.

Tapley, B.D., Bettadpur, S., Watkins, M., Reigber, C. (2004). The gravity recovery and climate experiment: mission overview and early results, Geophysical Research Letters, 31, L09607, doi: 10.1029/2004GL019920.

Tippett, M.K., Anderson, J.L., Bishop, C.H., Hamill, T.M., Whitaker, J.S. (2003). Ensemble square root filters, Mon. Weath. Rev., 131, 148590.

Tourian, M.J., Elmi, O., Chen, Q., Devaraju, B., Roohi, Sh., Sneeuw, N. (2015). A spaceborne multisensor approach to monitor the desiccation of Lake Urmia in Iran, Remote Sensing of Environment, Volume 156, January 2015, Pages 349-360, ISSN 0034-4257, https://doi.org/10.1016/j.rse.2014.10.006.

Tregoning, P., McClusky, S., van Dijk, A.I.J.M., Crosbie, R.S., Pea-Arancibia, J.L. (2012). Assessment of GRACE satellites for groundwater estimation in Australia, Waterlines report, National Water Commission, Canberra.

Trigo, R.M., Gouveia, C.M., Barriopedro, D. (2010). The intense 20072009 drought in the Fertile Crescent: Impact and associated atmospheric circulation, Agric. For. Meteorol., 150, 12451257.

Tropical Rainfall Measuring Mission (TRMM), (2011). TRMM (TMPA/3B43) Rainfall Estimate L3 1 month 0.25 degree x 0.25 degree V7, Greenbelt, MD, Goddard Earth Sciences Data and Information Services Center (GES DISC), Accessed [Data Access Date] https://disc.gsfc.nasa.gov/datacollection/TRMM_3B43_7.html.

United Nations (2015). United Nations Department of Economic and Social Affairs. World Population Prospects: The 2015 Revision.

Van Camp, M., Radfar, M., Martens, K., Walraevens, K. (2012). Analysis of the groundwater resource decline in an intramountain aquifer system in Central Iran. Geologica Belgica, 15/3, 176180.

van Dijk, A.I.J.M. (2010). The Australian Water Resources Assessment System: Technical Report 3, Landscape model (version 0.5) Technical Description, CSIRO: Water for a Healthy Country National Research Flagship.

van Dijk, A.I.J.M., Renzullo, L.J., and Rodell, M. (2011). Use of Gravity Recovery and Climate Experiment terrestrial water storage retrievals to evaluate model estimates by the Australian water resources assessment system, Water Resour. Res., 47, W11524, http://dx.doi.org/10.1029/2011WR010714.

van Dijk, A.I.J.M., Pea-Arancibia, J.L., Wood, E.F., Sheffield, J., Beck, H.E. (2013). Global analysis of seasonal streamflow predictability using an ensemble prediction system and observations from 6192 small catchments worldwide, Water Resour. Res., 49, 27292746, http://dx.doi.org/10.1002/wrcr.20251.

van Dijk, A.I.J.M., Renzullo, L.J., Wada, Y., Tregoning, P. (2014). A global water cycle reanalysis (20032012) merging satellite gravimetry and altimetry observations with a hydrological multi-model ensemble. Hydrol Earth Syst Sci 18:29552973, http://dx.doi.org/10.5194/hess-18-2955-2014.

Voss, K.A., Famiglietti, J.S., Lo, M.-H., de Linage, C., Rodell, M., Swenson, S.C. (2013). Groundwater depletion in the Middle East from GRACE with implications for transboundary water management in the TigrisEuphratesWestern Iran region. Water Resources Research, 49, http://dx.doi.org/10.1002/wrcr.20078.

Vrugt, J.A., ter Braak, C.J.F., Diks, C.G.H., Schoups, G. (2013). Advancing hydrologic data assimilation using particle Markov chain Monte Carlo simulation: theory, concepts and applications, Advances in Water Resources, Anniversary Issue - 35 Years, 51, 457-478, http://dx.doi.org/10.1016/j.advwatres.2012.04.002.

Wahr, J.M., Molenaar, M., Bryan, F. (1998). Time variability of the Earth's gravity field: hydrological and oceanic effects and their possible detection using GRACE. J Geophys Res 108(B12):3020530229, http://dx.doi.org/10.1029/98JB02844.

Whitaker, J.S., Hamill, T.M. (2002). Ensemble data assimilation without perturbed observations, Mon. Wea. Rev., 130, 1913 1924.

Wolf, A.T., Newton, J.T. (2007). Case study transboundary dispute resolution: The Tigris-Euphrates Basin, Transboundary Freshwater Dispute Database (TFDD), Oregon State University, http://www.transboundarywaters.orst.edu/.

Zaitchik, B.F., Rodell, M., Reichle, R.H. (2008). Assimilation of GRACE terrestrial water storage data into a land surface model: results for the Mississippi River Basin. J Hydrometeorol 9(3):535548, http://dx.doi.org/10.1175/2007JHM951.1.

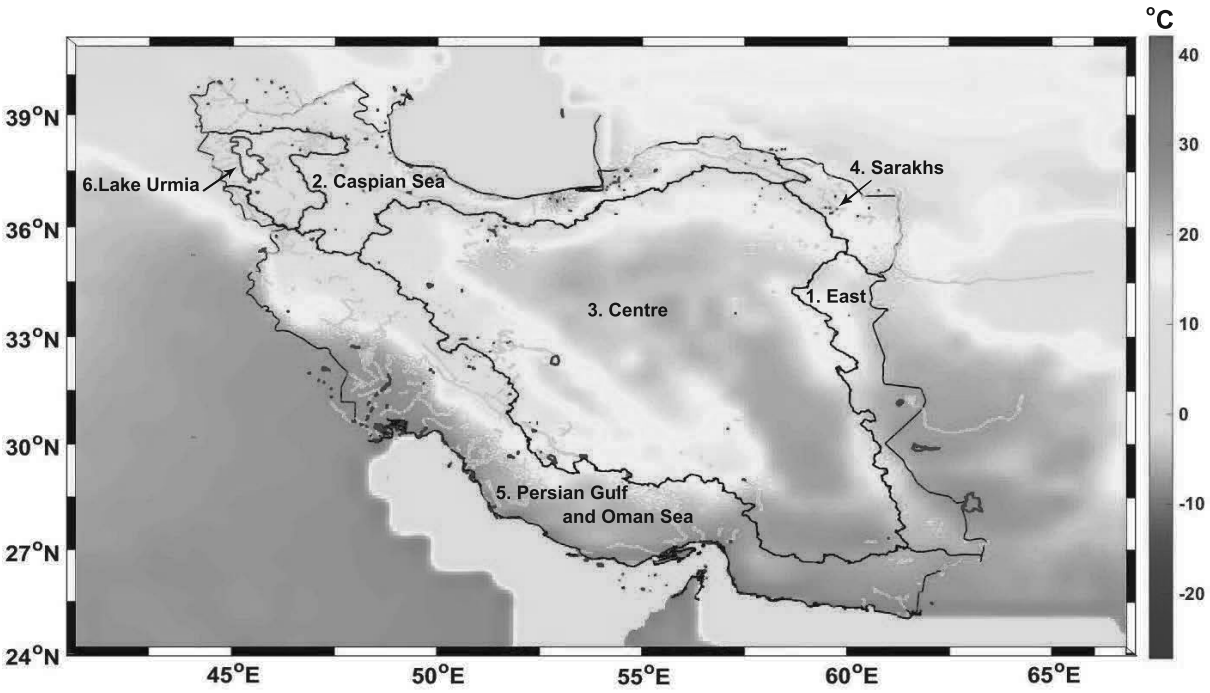

Figure 1: The study area and its average temperature (Harris, 2008). The figure also contains the locations of 6 major catchments separated by black solid lines.

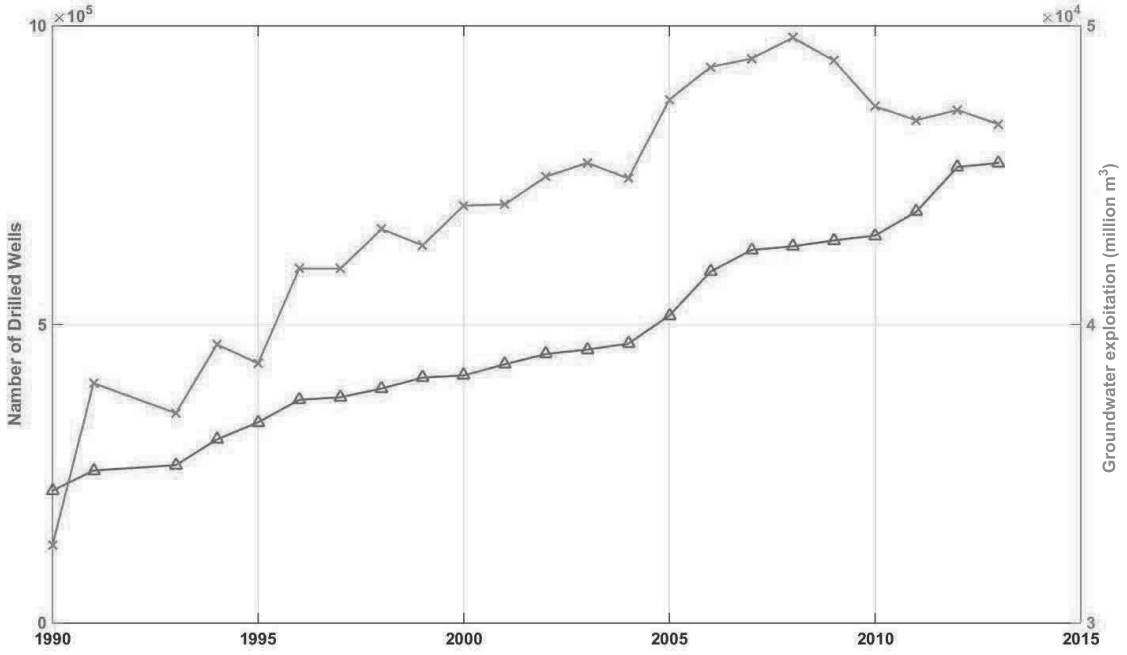

Figure 2: Groundwater depletion and the number of drilled wells in Iran from IWRMC.

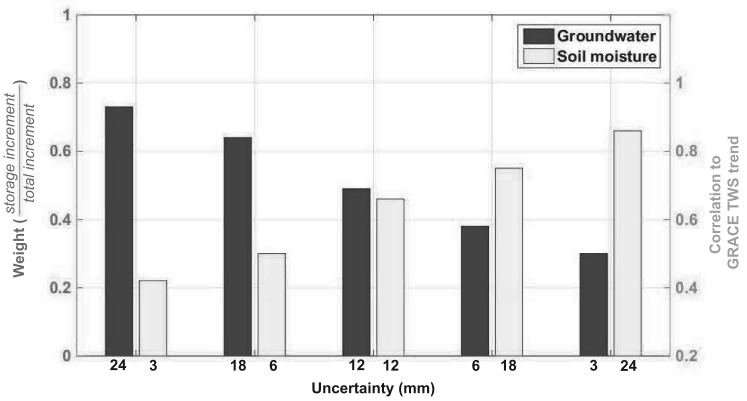

Figure 3: Relationships between groundwater and soil moisture state variable uncertainties and corresponding weights during data assimilation.

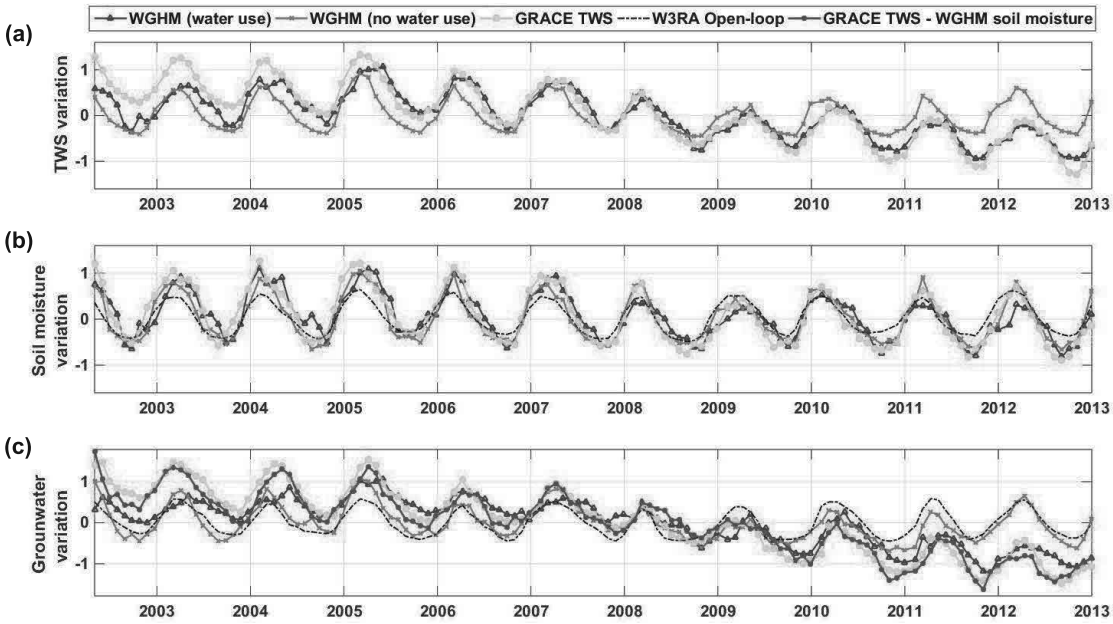

Figure 4: (a) Simulated average TWS observations using WGHM with and without human use, and W3RA open-loop plus GRACE trend. Average soil moisture (b) and groundwater (c) estimates from data assimilation based on simulated observations in (a).

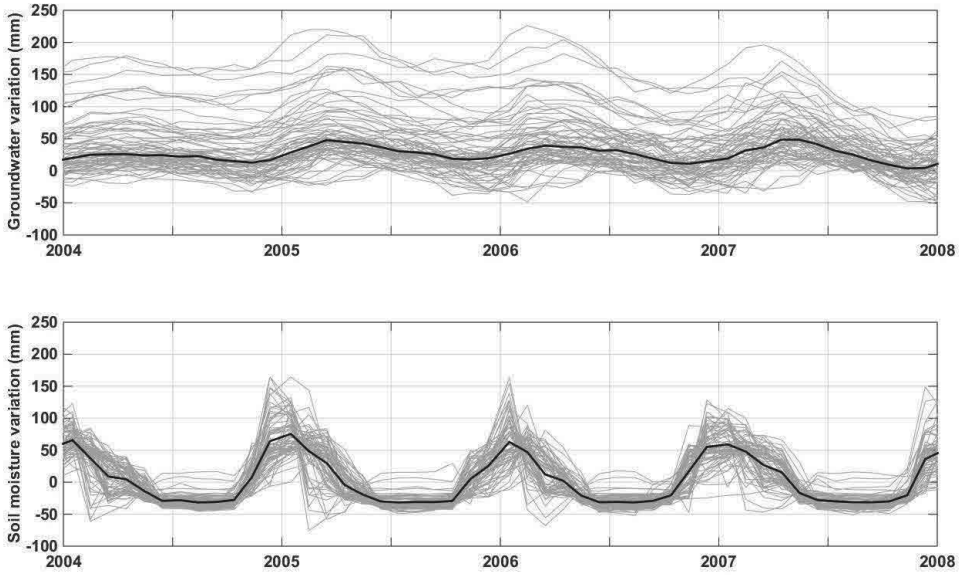

Figure 5: Average groundwater and soil moisture ensemble spreads between 2004 and 2008 over Iran. Gray lines indicate ensemble members and the black solid line present ensemble mean. Larger ensemble propagation is evident compared to that of soil moisture that represents larger uncertainties in the former water storage compartment.

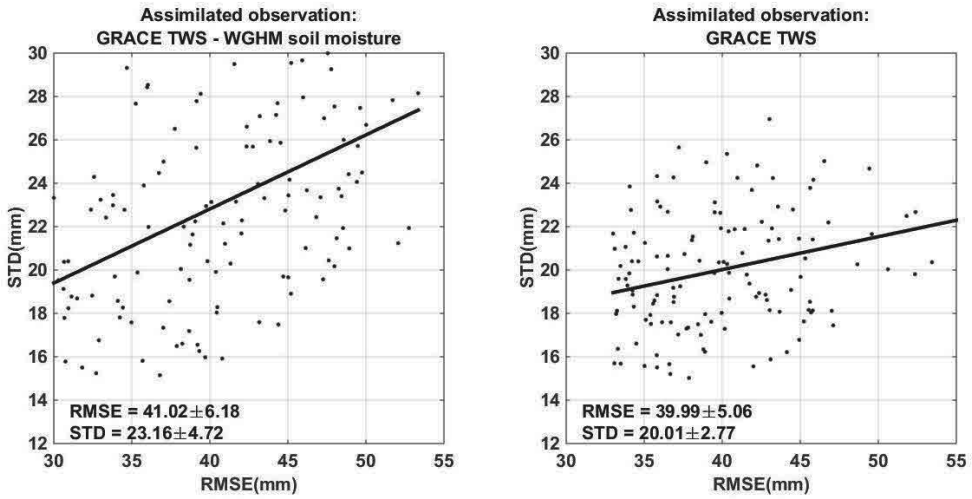

Figure 6: Average groundwater RMSE and STD from assimilating GRACE TWS and GRACE TWS minus soil moisture.

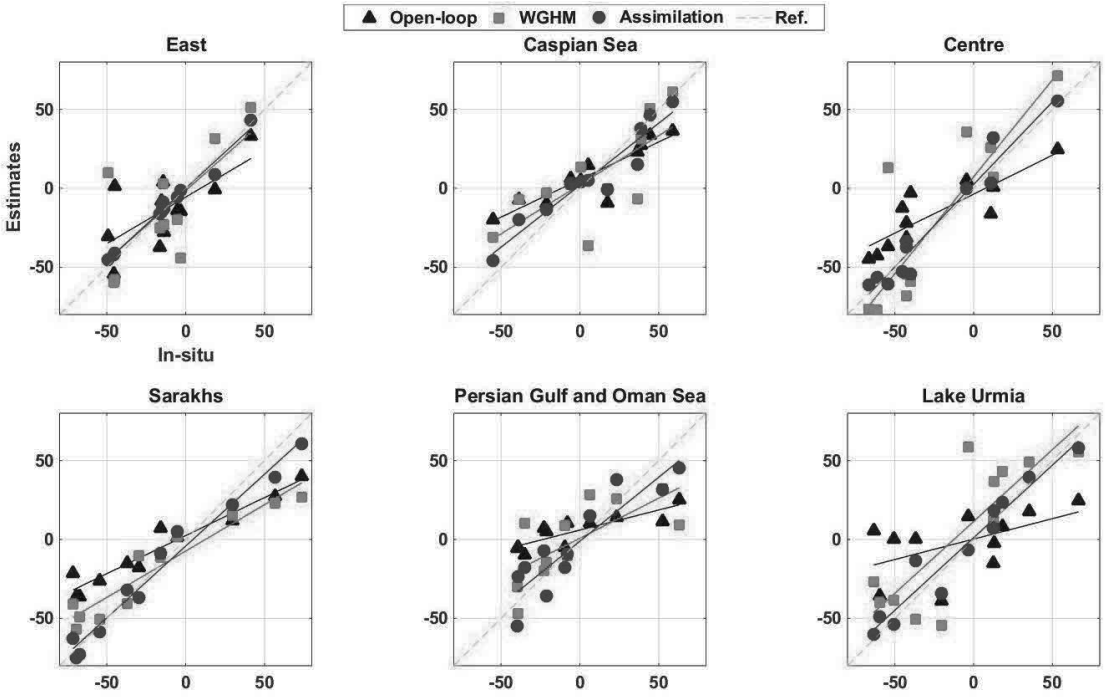

Figure 7: Comparison between in-situ groundwater measurements and those estimated by open-loop run, data assimilation, and WGHM over different catchments (units are mm).

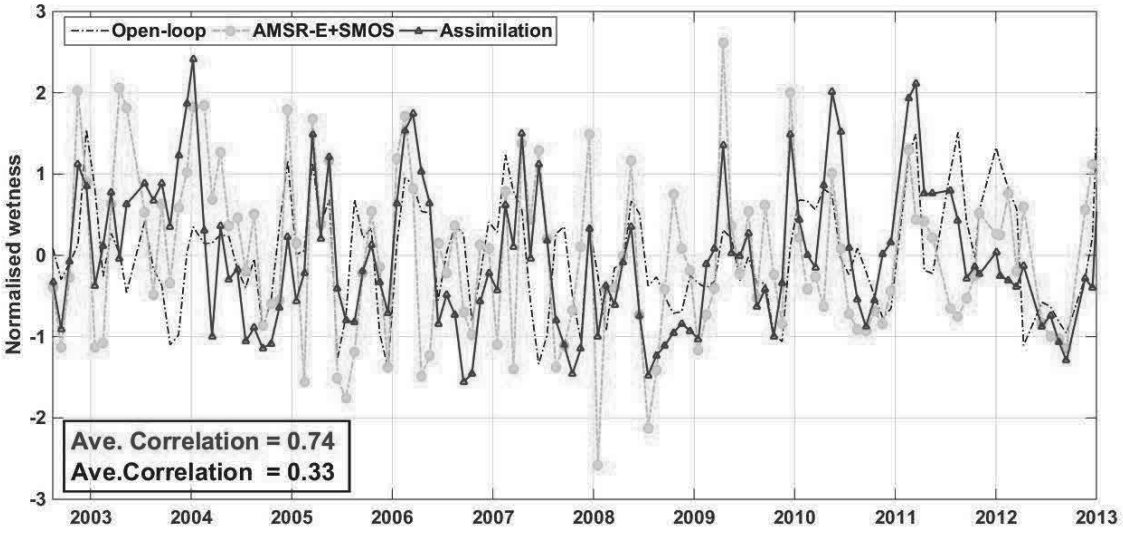

Figure 8: Comparison between the average estimated top layer soil moisture with and without (open-loop) data assimilation and soil moisture observations from satellite remote sensing (AMSR-E+SMOS). Correlations between the satellite measurements and both open-loop and assimilation estimates are also repotted in the figure.

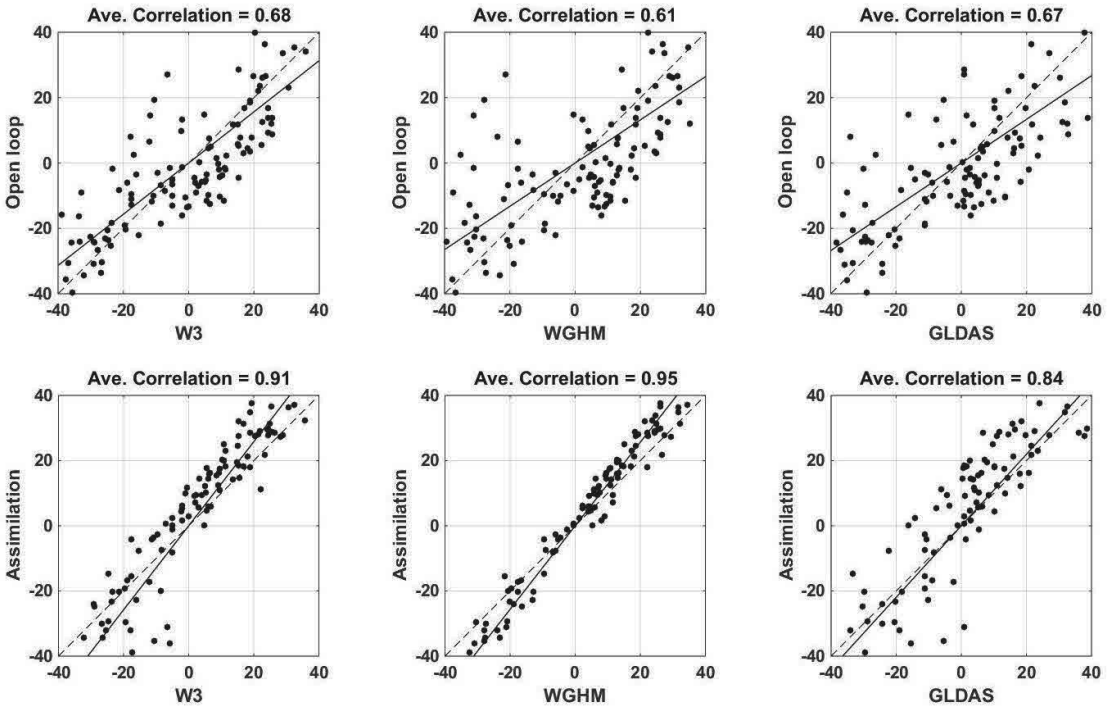

Figure 9: Comparison between the average soil moisture estimates from open-loop and data assimilation, and soil moisture products of W3, WGHM, and GLDAS (units are mm).

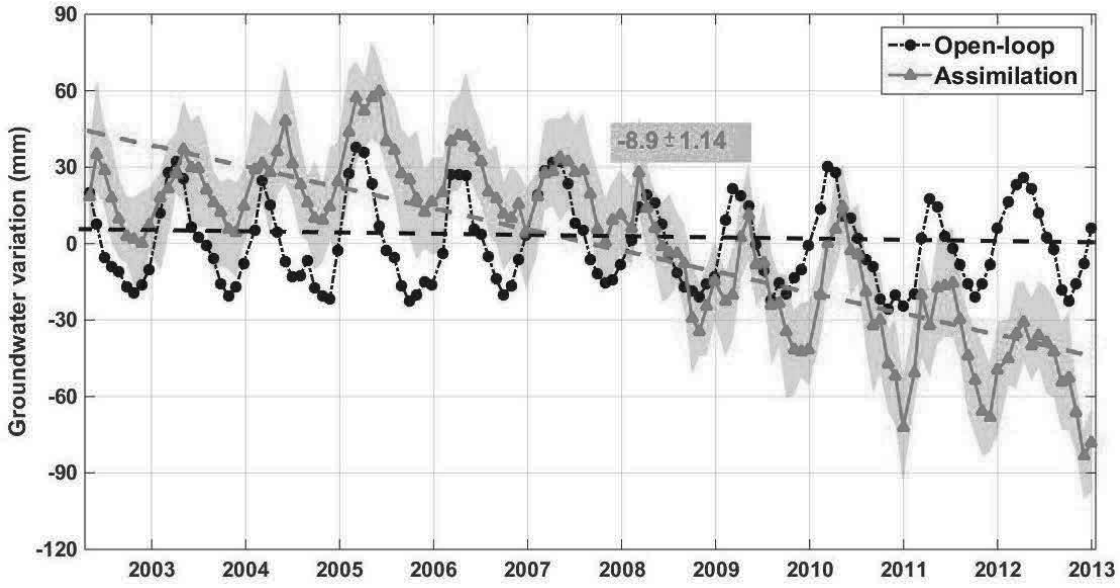

Figure 10: Average groundwater variations within Iran from open-loop and data assimilation results and corresponding 95% confidence intervals (shaded blue). Trend lines for time series are also displayed by dashed lines. Note that the open-loop time series slop is not reported because no significant trend is observed.

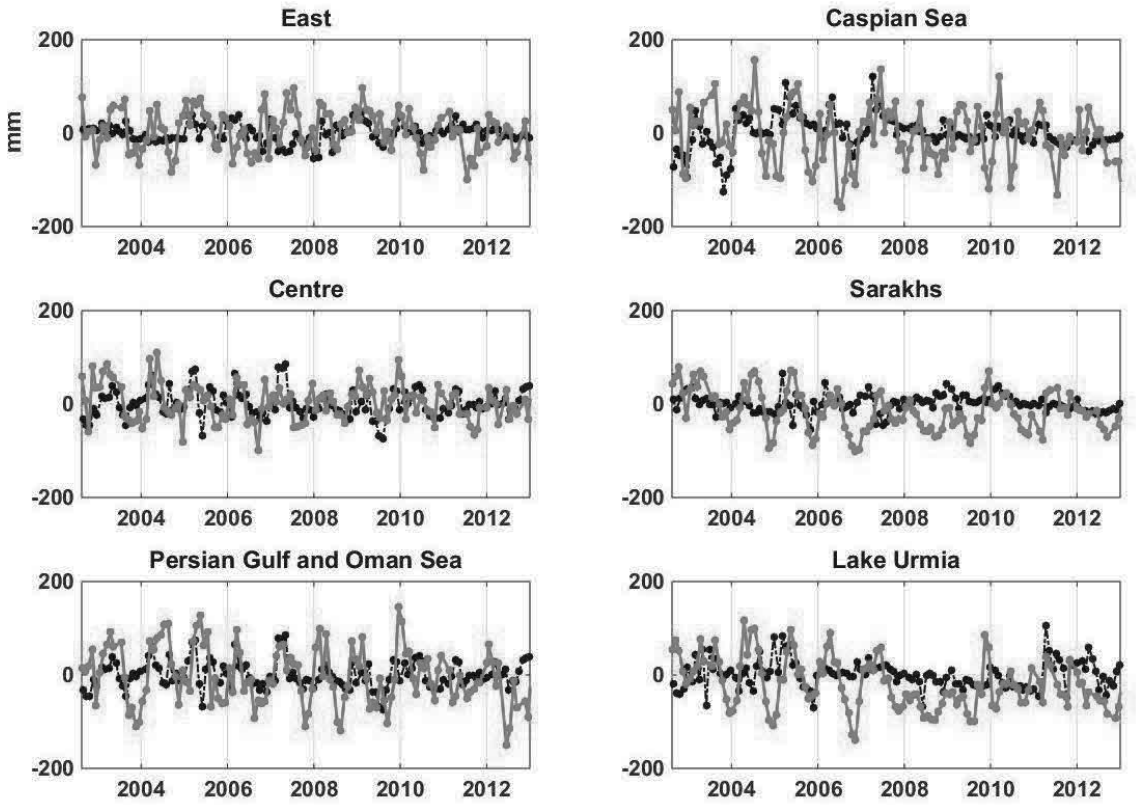

Figure 11: Average time series of soil moisture variations over different catchments with (blue) and without (black) data assimilation.

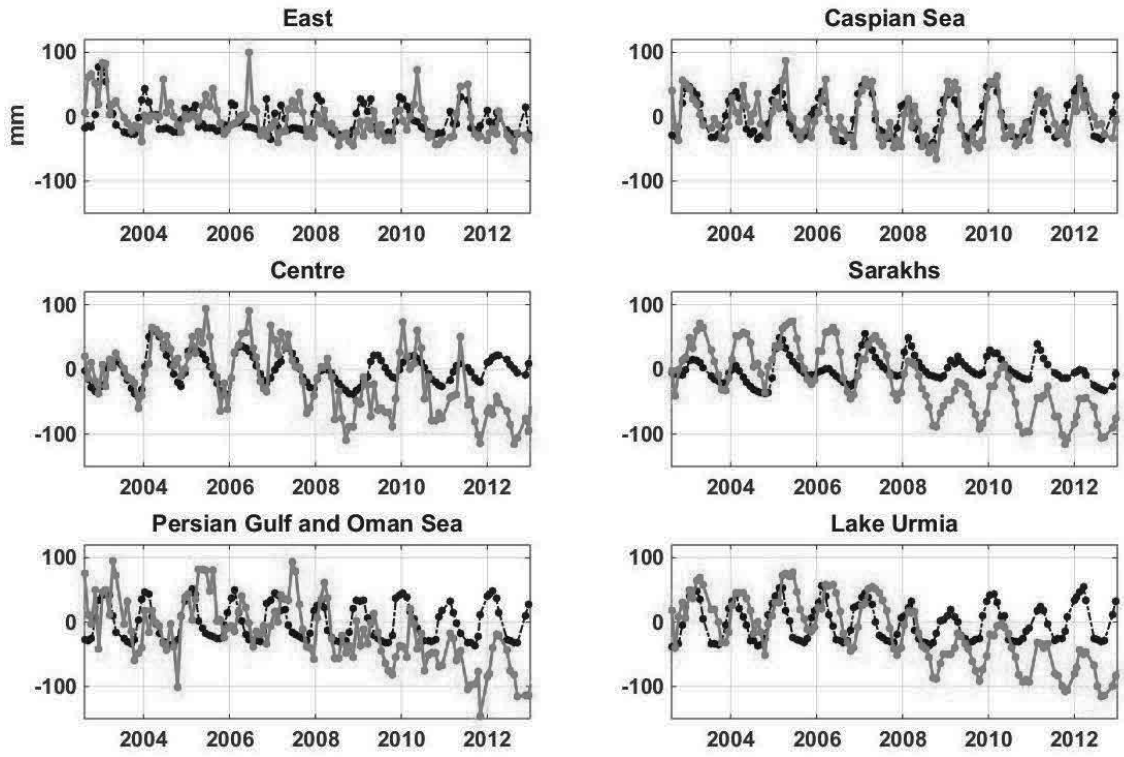

Figure 12: Average time series of groundwater variations over different catchments with (blue) and without (black) data assimilation. The correlations of time series with the in-situ measurements, as well as the trends of assimilation results are reported in Table 2.

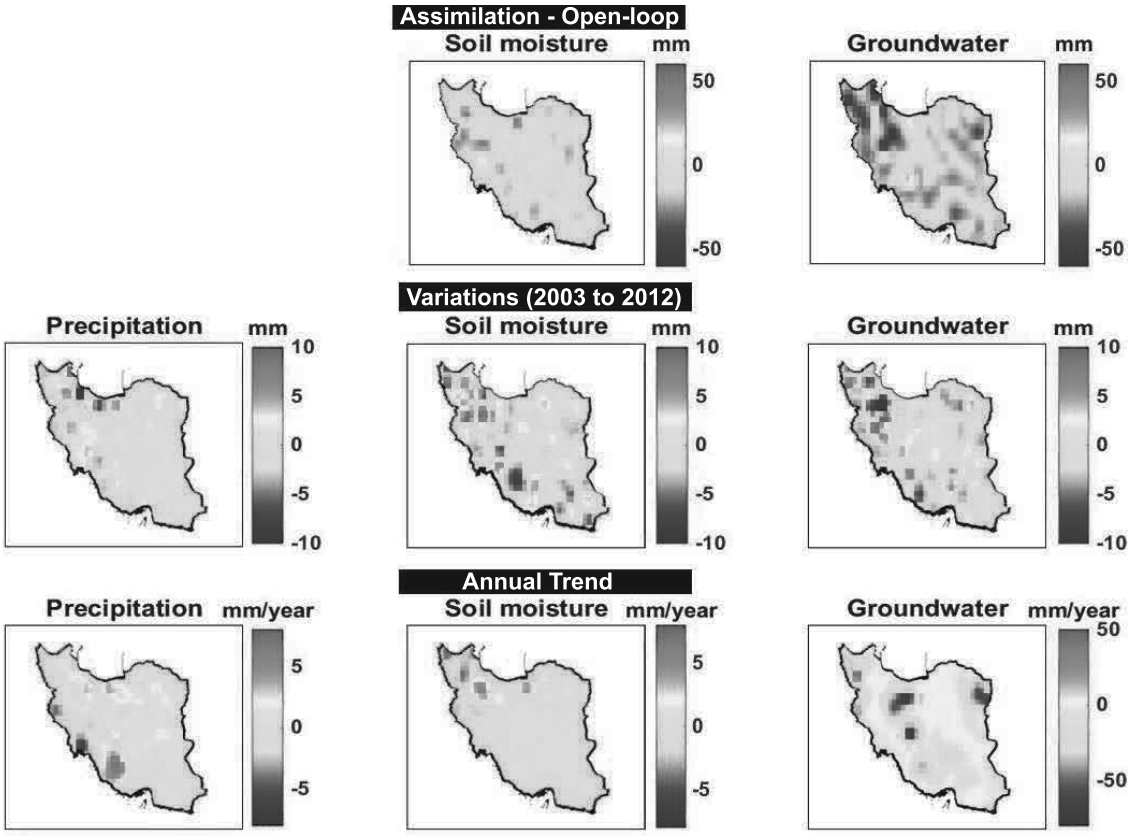

Figure 13: First row: temporally averaged increments applied to soil moisture and groundwater storages. Second row: variation of precipitation, soil moisture, and groundwater (after data assimilation) estimated as the average of each time series at each grid point. Third row: gridded trend of time series precipitation, soil moisture, and groundwater (after data assimilation) time series.

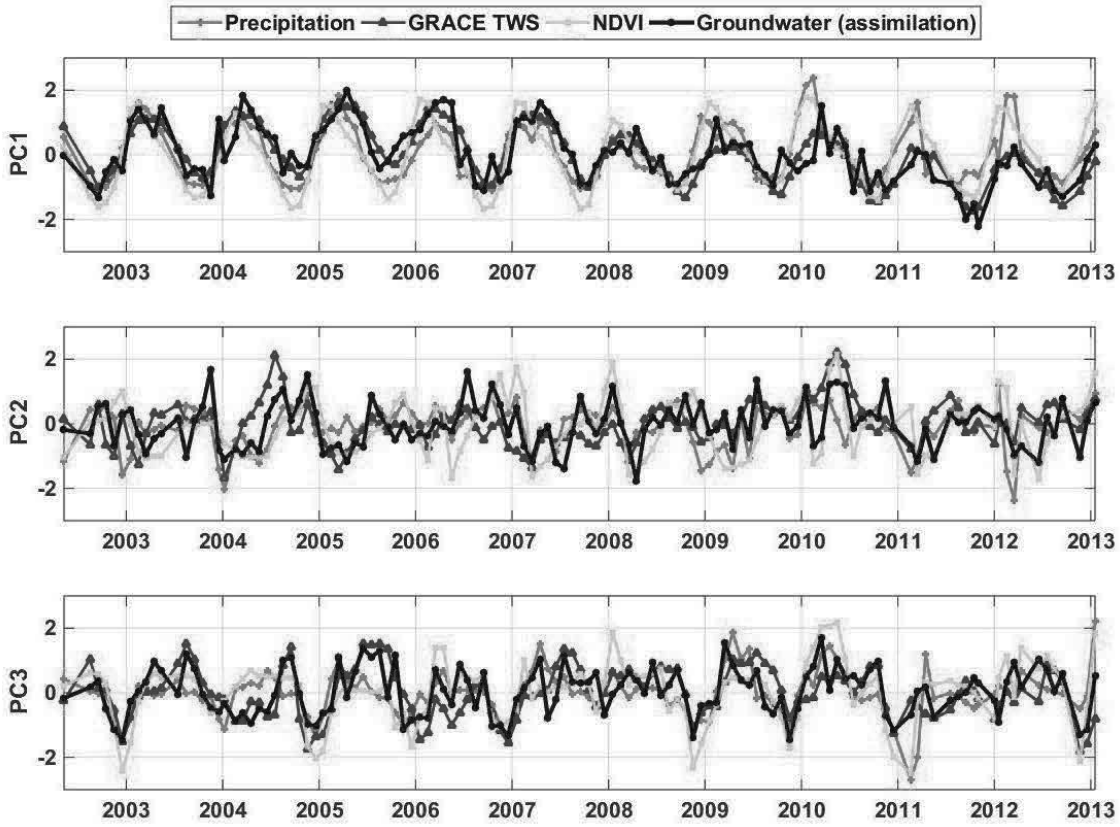

Figure 14: The three first principal components of precipitation, GRACE TWS, NDVI, and groundwater.

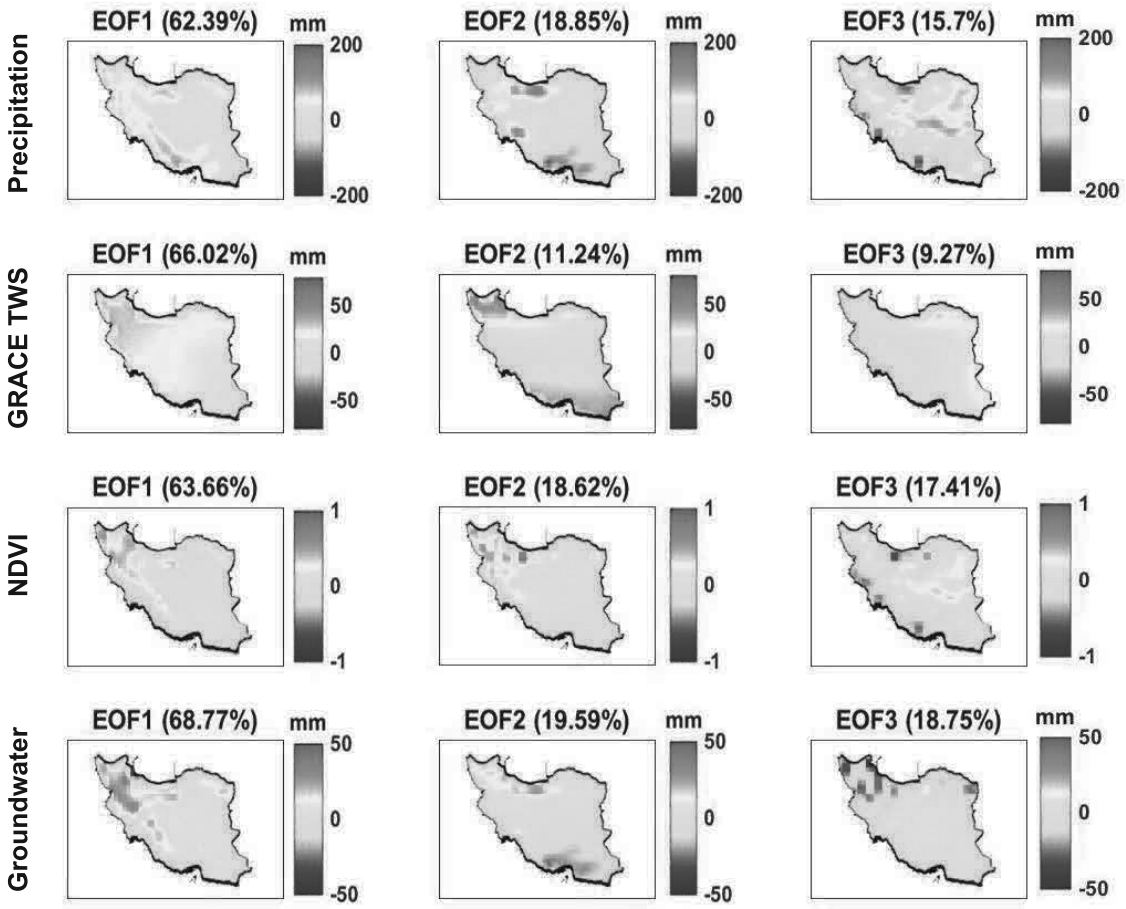

Figure 15: The empirical orthogonal functions (EOF1, EOF2, and EOF3) extracted from precipitation, GRACE TWS, NDVI, and groundwater.

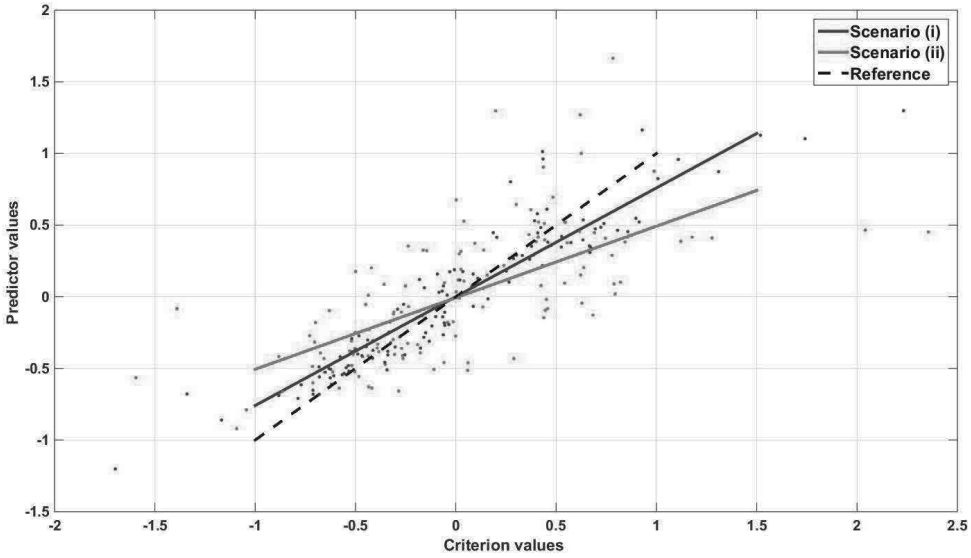

Figure 16: Scatter bi-plots (circles) and the linear trend (solid lines) of average canonical coefficients from CCA for each scenario applied. The combination of the water storages and discharge data and their canonical coefficients are in the x-axis (as criterion variables), the y-axis represents the combination of the predictor variables. Black solid line represents the reference line.

Table 1: A summary of the datasets used in this study.

Description	**Platform**	**Data access**
Terrestrial water storage (TWS)	GRACE	https://www.tugraz.at/institute/ifg/downloads/gravity-field-models/itsg-grace2014/
Precipitation	TRMM-3B43	https://disc.gsfc.nasa.gov/datacollection/TRMM_3B43_7.html
Normalized Difference Vegetation Index (NDVI)	NASA-GSFC	ftp://eclipse.ncdc.noaa.gov/pub/cdr/avhrr-land/ndvi/
Hydrological model	W3RA	http://www.wenfo.org/wald/data-software/
Temperature	Harris (2008)	https://crudata.uea.ac.uk/cru/data/hrg/
Groundwater in-situ measurements	IWRMC	http://www.wrm.ir/
Average water consumption	IWRMC	http://www.wrm.ir/
Discharge data	IWRMC	http://www.wrm.ir/
Number of groundwater bore holes	IWRMC	http://www.wrm.ir/
Altimetry-derived level height	Jason-1	http://podaac.jpl.nasa.gov
Altimetry-derived level height	Jason-2	http://avisoftp.cnes.fr/

Table 2: The undertaken experiments and corresponding research objectives. The result section associated to each experiment is also presented.

Experiment	**Research objective**	**Result section**
Simulated assimilation	To assess the impacts of GRACE observations on different water storage	Section 4.1
Evaluation procedure	To examine the validity of results against independent observations	Section 4.2
Water storage analysis	To analyze spatio-temporal variations of groundwater and soil moisture	Section 4.3
Climatic impacts using PCA	To investigate the impacts of climate indicators (e.g., precipitation) on water storage	Section 4.4
CCA	To establish the relations between water storages and human- as well as climate-related variables	Section 4.5

Table 3: Statistics of groundwater variations and its errors with respect to the in-situ observations. For each region the RMSE average and its range (±XX) at the 95% confidence interval is presented. Improvements in data assimilation results are calculated for each catchment in relation to the water storages from the model without implementing data assimilation.

		Assessment with In-situ				
		Open-loop		Assimilation		
Region	Groundwater trend (mm/year)	Correlation	RMSE (mm)	Correlation	RMSE (mm)	Improvement (%)
East	-3.8	0.57	60±8.66	0.84	38±4.64	36.29
Caspian Sea	-2.1	0.64	64±9.19	0.73	46±5.13	28.13
Centre	-6.7	0.63	55±7.84	0.65	41±5.01	26.55
Sarakhs	-5.4	0.61	52±7.58	0.82	32±4.26	38.64
Persian Gulf and Oman Sea	-9.3	0.56	79±9.07	0.75	49±5.17	37.81
Lake Urmia	-11.8	0.52	69±8.28	0.81	40±4.25	41.90

Table 4: Average canonical correlation coefficients and variable loadings for the data inputs in CCA for each scenario.

			Scenario (i)	**Scenario (ii)**
			Canonical coefficients	**Canonical coefficients**
Canonical correlation coefficient			0.972	0.841
Predictor variables	Water use for:	Precipitation	0.721	0.749
		NDVI	0.365	0.412
		Temperature	-0.591	-0.681
		# Farming	-0.938	–
		# Industry	-0.758	–
		# Drink (Urban use)	-0.820	–
		Number of bore holes	-0.893	–
Criterion variables		Groundwater	0.938	0.705
		Soil moisture	0.633	0.617
		Water discharge	0.174	0.249